Agency/Office/Program	DOE/EERE/Solar Energy Technology Office	
Award Number	DE-EE0008981	
Project Title	Technoeconomic Analysis of Novel PV Plant Designs for Extreme Cost Reductions	
Principal Investigator	Robin Bedilion Principal Technical Leader rbedilion@epri.com 509-714-1766	
Business Contact	Bethany Thompson bthompson@epri.com 865-218-5925	
Submission Date	September 28, 2021	
DUNS Number	062511126	
Recipient Organization	Electric Power Research Institute, Inc. (EPRI)	
Project Period	**Start:** 04/01/2020	**End:** 06/30/2021
Project Budget	Total: $249,957 (DOE: $199,965; C/S: $49,992)	
Submitting Official Signature	Electronic signature (i.e., Adobe Acrobat)	

Acknowledgement: This material is based upon work supported by the U.S. Department of Energy's Office of Energy Efficiency and Renewable Energy (EERE) under the Solar Energy Technologies Office (SETO) Award Number DE-EE0008981.

Executive Summary:

Solar photovoltaic (PV) costs have declined considerably over the past decade, the bulk of which can be attributed to cost reductions and efficiency improvements of PV modules. More efficient modules also reduce the amount of land and racking and mounting equipment required, bringing down the overall plant cost per Watt-DC. However, cost reductions and efficiency improvements in traditional crystalline silicon (c-Si) PV modules are anticipated to asymptote, leading to research focused on other individual aspects of plants, including new PV cell and module technologies to further increase efficiency and power output and increased voltages and module-level power electronics for reduced energy loss. More research is needed on how these individual innovations can best come together to provide the lowest cost PV electricity and to understand the design trade-offs that balance cost, power output, and reliability to achieve the lowest levelized cost of electricity (LCOE).

This project sought to gain a deeper understanding of the cost and performance of future PV plant components, including bifacial PV modules, tandem PV modules, increased plant voltage architectures, and module-level power electronics, and how they may be integrated into new PV plant designs to significantly reduce the LCOE of PV. This was done through extensive modeling of current PV plants and future technologies in three different locations, informed by a comprehensive literature review and informational interviews to develop performance and cost assumptions for these technologies. Sensitivities were conducted to understand tradeoffs between different design options, such as the added energy from increasing row spacing versus additional land costs. An optimization tool was then created utilizing an evolutionary algorithm to determine an optimal PV plant configuration for a given set of technologies that resulted in minimized plant LCOE based upon typical performance and cost inputs.

Three of the four technologies evaluated – bifacial modules, tandem modules, and increased plant voltages – resulted in increased plant output compared to the baseline plants and, in optimized cases, potential reductions in LCOE when compared to current baseline LCOEs. This project demonstrated the importance of a coordinated strategy between novel PV technologies and plant design considerations such as ground coverage ratio, module ground clearance height, and albedo when trying to achieve LCOE reductions for PV plants.

The optimization tool developed through this project for use with the National Renewable Energy Laboratory (NREL) System Advisor Model (SAM) has been published publicly on GitHub to support further research around PV plant optimization. Results are also being communicated through industry conferences and stakeholder meetings. By communicating the results of this effort with the broader PV community, future demonstration and development of PV technologies and plant designs can focus on those areas of greatest impact.

Table of Contents:

Background:

Utility-scale deployment of the technologies investigated in this project, namely bifacial modules, tandem modules, increased voltage (1500V+) architectures, and module-level power electronics (MLPE), is relatively new or has not begun. As such, the state-of-the-art of these technologies is continuing to evolve. Ongoing research and publications around these technologies has helped guide this project research.

Research by Patel et al. (2019 & 2020) [1][2] describing the temperature effects of increased bifacial module racking height, citing an energy gain of 1-15% between bifacial modules mounted at 2 m versus grade height (0 m) has informed assumptions around the optimization of ground clearance height for bifacial modules. Research by Marion et al. (2017) [3] showing negligible increased backside irradiance for end-of-row modules in bifacial installations of more than a dozen PV modules per row helped to inform additional bifacial modeling assumptions. Solar manufacturers also continued to update their bifacial module offerings over the course of the project, with LONGi Group releasing their HiMO5 bifacial module, with front-side power up to 540W and efficiencies above 21% [4] followed by Canadian Solar's launch of their Series 7 bifacial modules, rated for up to 665W and 21.5% efficiency [5]. These recent launches informed bifacial module selection and analyses in this study.

For tandem modules, early research by Etxebarria et al. (2014) [6] and White et al. (2014) [7] highlighted advantages and disadvantages of different terminal configurations for tandem modules and considerations for how to achieve low-cost, high-efficiency tandem modules, supporting technology selection and modeling approaches within the project. Recently, efficiency records have been broken for perovskite/silicon tandem solar cells, approaching 30% for small-scale cells (~1 cm^2) [8]. A monofacial four-terminal (4T) tandem module efficiency of 26.5% reported by Coletti et al. (2020) [9] was used as a reference to establish a scale factor between a baseline c-Si module and a tandem module, while cost information reported by Sofia et al. (2019) [10] informed cost development assumptions.

Research by West (2011) [11] and Scarpa et al. (2018) [12] investigated environments above $1500V_{DC}$, highlighting key issues needing to be addressed by international standards to achieve increased voltage configurations.

MLPE research by Deline et al. (2012) [13] investigated the effects of PV plant shading and the potential increases in production that MLPE could provide. Earlier work by Elasser et al. (2010) [14] concluded that though MLPE can be effective for improved energy yield, it is more cost effective for commercial applications than for utility-scale applications, though this conclusion was based on MLPE cost at the time of publication. Further MLPE research by Vinnikov et al. (2019) [15] describes both the concept of a solar optiverter (combining the benefits of a DC optimizer with a microinverter) and the pros and cons of microinverters and DC optimizers. This research was used to inform modeling assumptions and consideration around MLPE implementation.

Project Objectives:

Solar PV has experienced a precipitous decline in costs over the past decade, the bulk of which can be attributed to cost reductions and efficiency improvements of PV modules.

More efficient modules also reduce the needed amount of land and racking and mounting equipment, bringing down the overall plant cost per Watt-DC. However, with the cost of PV modules falling below $0.30/W$_{DC}$ globally and efficiencies of c-Si cells approaching theoretical limits, cost reductions and efficiency improvements in traditional c-Si PV modules are anticipated to asymptote. In an effort to continue decreasing cost trends, research has focused on other individual aspects of plants, including new PV cell and module technologies to further increase efficiency and power output, and increased voltages and module-level power electronics for reduced energy loss. However, more research is needed on how these individual innovations can best come together to provide the lowest cost PV electricity. As with other increasingly constrained and optimized systems, trade-offs need to be made. For PV plants, technology selection decisions balance cost, power output, and reliability to achieve the lowest LCOE. It is not readily apparent how low of a LCOE can be achieved by any given combination of technologies.

There are two broad areas for opportunity for innovation in PV plant design. The first is improvements in the individual components that make up a PV plant. The second opportunity for reducing cost through PV plant design is in optimizing the integration of the plant components as a whole. This project sought to gain a deeper understanding of the cost and performance of future PV plant components, including bifacial PV modules, tandem PV modules, increased plant voltage architectures, and module-level power electronics, and how they may be integrated into new PV plant designs to significantly reduce the LCOE of PV. This was done through extensive modeling of current PV plants and future technologies in three different locations, informed by a comprehensive literature review and informational interviews to develop performance and cost assumptions for these technologies. An optimization tool was then created utilizing an evolutionary algorithm to determine an optimal PV plant configuration for a given set of technologies that resulted in minimized plant LCOE based upon typical performance and cost inputs, with a goal of identifying an optimized set of technologies and plant configuration that led to a 20% or greater reduction in LCOE from the baseline costs. By communicating the results of this effort with the broader PV community, future demonstration and development of PV technologies and plant designs can focus on those areas of greatest impact.

The project set out to achieve these goals through several project tasks and sub-tasks, summarized briefly below:

Task 1.0: Modeling Baseline: PV plant performance and project economics will be modeled in NREL's SAM software.

***Subtask 1.1: PV Plant Performance Baseline*:** Three existing PV plants will be modeled in SAM to ensure the plant performance model accurately captures actual plant performance. These same plants will then be utilized in Task 3.0 to allow for an accounting of actual project performance against the performance new technologies might offer. (Milestone 1.1: Modeled power production <10% discrepancy)

***Subtask 1.2: PV Plant Economic Baseline*:** The economic performance of the three PV plants modeled in Subtask 1.1 will be modeled utilizing NREL's SAM model. Representative cost and equipment performance will be captured, but agreement error

between the model and final cost of the three real plants may be higher than performance modeling due to particular financial arrangements for the plants for which EPRI will not have the details. (Milestone 1.2: Modeled plant economics <25% discrepancy)

Task 2.0: Technology Cost and Performance Discovery: To best determine the cost and performance of technologies that either do not yet exist or are in early stages of commercialization, a literature review and a series of informational interviews will be conducted with relevant technology experts at national laboratories, academia, and industry. The technologies and associated performance considerations to be explored are listed in the table below, along with modeling simplifications that may be required in order to capture the performance of these technologies without significant modification to NREL's SAM model.

Table 1. PV Plant Technologies for Exploration and Associated Design Considerations

PV Plant Technology	Example Plant Design Trade-Offs	Example Modeling Simplifications
Bifacial modules	Added energy from increasing module height vs. increased racking and wiring cost; added energy from increasing ground albedo vs. cost of solution	Constant albedo across plant site during all seasons; backside capture uniform across string length
Tandem modules	Added energy from increasing efficiency vs. increased wiring and balance-of-plant costs	Light capture/ performance same as c-Si for both layers; cells wired in series
Increased plant voltage (1500+ V)	Reduced energy losses vs. increased component costs	Mounting same as low voltage; cable material properties scale proportionally
Module-level power electronics for large-scale plants	Reduced energy losses and potential for lower cost inverters vs. increased upfront and maintenance costs	No mounting impact; no impact on string length

***Subtask 2.1: Literature Review*:** To determine the potential technical and economic performance of the innovations to be explored, an extensive literature review will be conducted. (Milestone 2.1: >40 technical papers reviewed)

***Subtask 2.2: Informational Interviews*:** To determine the potential technical and economic performance of the innovations to be explored, informational interviews will be conducted with relevant technology experts at national laboratories, academia, and industry. (Milestone 2.2: >16 informational interviews conducted)

Task 3.0: PV Plant Modeling Optimization: With the models validated in Task 1 and the data collected in Task 2, the PV plant technologies identified in Table 1 will be modeled at the three locations used in Task 1. Machine learning (ML) algorithms will then be employed to attempt to arrive at an optimal configuration that minimizes LCOE at each location.

***Subtask 3.1: PV Plant Performance Modeling*:** Using SAM and input gathered from Task 2, the power output from PV plants using the technologies highlighted in Table 1 will be modeled. Design of Experiment (DoE) methodology will be used to ensure that various plant design choices (e.g., string length, DC:AC ratio, ground coverage ratio) and technology combinations from Table 1 are modeled to capture any potential crossing effects between the technologies. (Milestone 3.1: Incorporation of new technologies into model)

***Subtask 3.2: PV Plant Economic Modeling*:** Using SAM and input gathered from Task 2, the economics of PV plants using the technologies highlighted in Table 1 will be modeled. Design of Experiment (DoE) methodology will be used to ensure that various technology combinations are modeled to capture any potential crossing effects between the technologies. (Milestone 3.1: Incorporation of new technologies into model)

***Subtask 3.3: PV Plant Optimization*:** To optimize PV plant economics with the number of new technologies that will be available, ML techniques are likely to be necessary. It is anticipated that employment of a genetic algorithm will be used to arrive at an optimal plant configuration for each of the three locations, but other potential ML techniques will be evaluated during the course of the work to arrive at an appropriate ML approach. (Milestone 3.2: Ability of model to run multiple runs and iteratively approach efficient frontier; Milestone 3.4: Model capable of multi-variate optimization)

Task 4.0: Improved Modeling of New Technologies: To improve the precision of the estimate of the future performance of bifacial modules and/or tandem cells, scripts will be created for use in SAM that more accurately capture specific performance characteristics of these new technologies.

***Subtask 4.1: Improved Modeling of Bifacial Modules*:** SAM will be modified to more accurately account for bifacial module performance. Example improvements include ability to account for seasonal variation in albedo and ability to account for shading variation across a row length. (Milestone 2.3: Modeling approach defined; Milestone 4.1: Demonstrated capability)

***Subtask 4.2: Improved Modeling of Tandem Modules (Stretch Subtask)*:** SAM will be modified to more accurately account for tandem module performance. Example improvements include ability to account for spectral absorbance and transmission difference between each layer and ability to string layers in parallel as well as series. Additionally, any changes in cost related to differing wire schemes will be captured and reflected in the technoeconomic analysis. (Milestone 4.2 (stretch): Demonstrated capability)

***Subtask 4.3: Re-run Plant Optimization (Stretch Subtask)*:** The plant optimization task will be re-run with the improved characterization of the technologies detailed in Subtask 4.1 and Subtask 4.2 *(stretch)*.

End of Project (EOP) Goal: The project seeks to gain a deeper understanding of the cost and performance of future PV plant components and how they may be integrated into new PV plant designs that significantly reduce the LCOE of PV, with a goal of >20% LCOE reduction being targeted as a threshold that will incentivize future research in the area. The results will be communicated broadly to the PV community so that future

demonstration and development of PV technologies and plant designs can focus on those areas of greatest impact. It is expected that the results of this work will be presented at various industry meetings, such as IEEE PVSC and/or SPI, in addition to EPRI meetings with utilities and a peer-reviewed, publicly available journal publication will be produced detailing the work. (Milestone 3.3: Acceptance into peer-reviewed journal; Milestone EOP-A: Modeled PV plant LCOE >20% reduction from baseline costs; Milestone EOP-B: Published optimization code)

Stretch End of Project (EOP) Goal: If time and budget permit, this project will seek to improve the performance modeling of bifacial modules and tandem cells in NREL's SAM. This work would either be released to the public via a code hosting site or given to NREL for direct incorporation into the SAM model.

Project Results and Discussion:

Task 1: Baseline Plant Modeling

PV Plant Performance Baseline

The first task in this project was the development of baseline models for plants in three different locations with varying plant configurations and weather profiles. To accurately calibrate each baseline model, plant data was gathered from three existing large-scale PV plants. Plants in the Southwest, the Southeast, and the Midwest were selected for baseline model development based on the reliability and duration of available plant data. These three plants, completed between 2014 and 2016, varied in plant size, module type, tracking technology, and inverter configuration, allowing for comparison of the impacts of the novel PV technologies explored in this study with several different existing technology types. Table 2 provides a high-level overview of the size and technologies of the three different plants.

Table 2: PV Plant Specifications.

	Southwest Plant	Southeast Plant	Midwest Plant
Approximate Plant Size	50 MW_{AC}	1 MW_{AC}	2.5 MW_{AC}
Module Type(s)	Cadmium telluride (CdTe), Multi c-Si	Mono c-Si	Multi c-Si
Tracking Type(s)	Single-axis tracking	Fixed-tilt, Single-axis tracking	Fixed-tilt
Inverter Type	Central	String	Central

To begin the baseline calibration, each plant was modeled using NREL's SAM model. Plants were modeled based on detailed plant configuration information and diagrams provided by the plant owners and compared with actual operating data for at least 12 months using weather data collected at the site. Site weather data was collected as plane of array (POA) irradiance data, which was run through SAM's decomposition algorithm to calculate diffuse horizontal irradiance (DHI) and direct normal irradiance (DNI) values. These values were then extracted and inserted into a custom weather file that could be used for future model simulations without need for POA decomposition during each model run.

For the Southwest and Southeast plants, which included a variety of array configurations with different module types or tracking systems, the plants were first modeled at the

inverter level, then at the array level, and finally summed to capture total plant performance. Starting at the inverter level helped to identify outliers within available plant data and improve model calibration by comparing modeled energy output with actual inverter-level plant energy yield on a monthly basis. Outliers due to identifiable weather anomalies, inverter outages, equipment failures, and data collection complications were filtered from recorded plant data, yielding adjusted monthly totals for each inverter. Once the inverter-level analysis and calibration was performed, array-level models were created and analyzed. The monthly modeled energy output and adjusted actual energy output for each array were then summed to arrive at total monthly energy output for the full plant. Figure 1 shows an overview of this methodology.

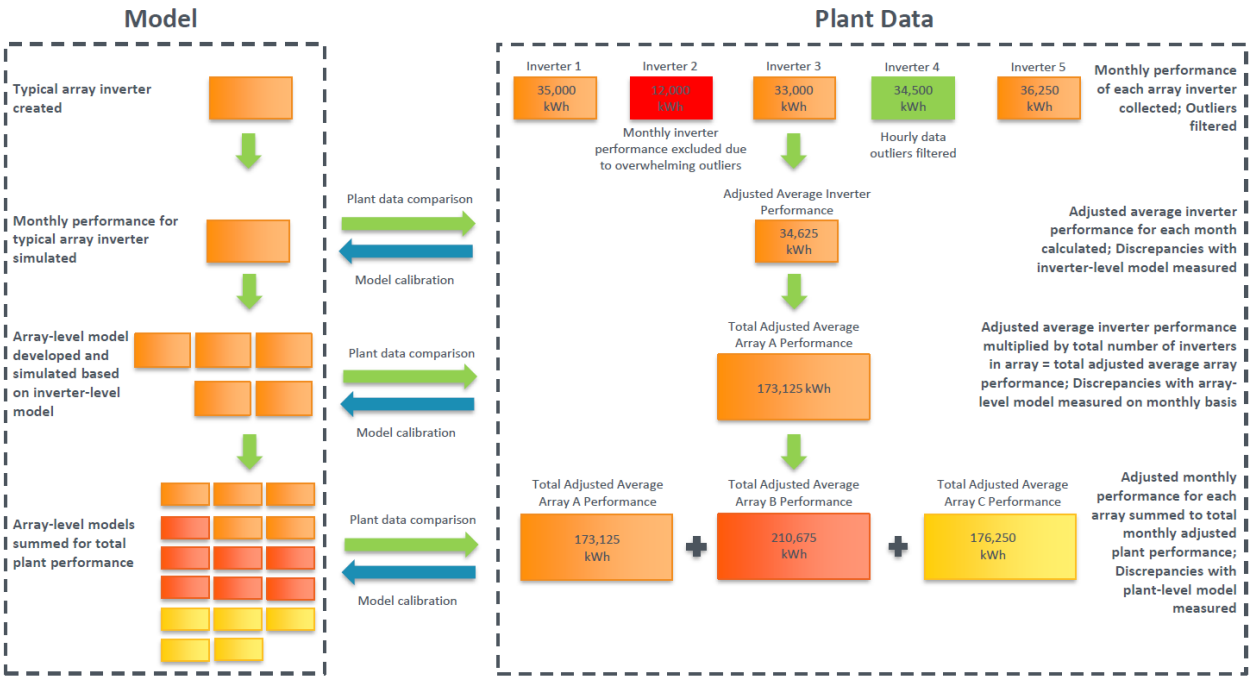

Figure 1: Model Calibration Methodology for the Southwest and Southeast Plants.

Table 3 and Figure 2 show the Southwest plant's Monthly Expected Energy calculated from the model compared with the Monthly Adjusted Actual Energy based on plant data, adjusted to remove anomalies. For each month of the nearly two-year analysis, as well as the total for each year, the Southwest plant SAM model had <10% discrepancy with actual plant data, satisfying the milestone success criteria and demonstrating a reasonable baseline model for moving forward with analysis.

Table 3: Comparison of Monthly Expected Energy and Adjusted Actual Energy for the Southwest Plant from 2015-2016.

2015	Month	Monthly Expected Energy (kWh)	Monthly Adjusted Actual Energy (kWh)	Percent Difference (%)
	February	9,483,930	9,270,935	2.3%
	March	12,851,090	13,050,269	-1.5%
	April	14,712,200	14,994,329	-1.9%

	May	16,087,070	15,282,798	5.3%
	June	15,055,570	15,826,526	-4.9%
	July	15,167,860	15,575,714	-2.6%
	August	14,576,790	14,973,080	-2.6%
	September	11,333,570	11,323,961	0.1%
	October	10,175,980	10,012,691	1.6%
	November	8,870,090	8,166,833	8.6%
	December	7,702,720	7,038,225	9.4%
	Total	136,016,870	135,515,360	0.4%
2016	January	7,379,320	7,252,189	1.8%
	February	10,246,290	10,601,557	-3.4%
	March	12,908,320	12,742,308	1.3%
	April	14,076,470	14,524,794	-3.1%
	May	17,082,120	17,116,446	-0.2%
	June	15,990,420	15,796,787	1.2%
	July	16,439,950	15,634,405	5.2%
	August	15,041,360	13,913,001	8.1%
	September	12,256,760	11,602,209	5.6%
	October	11,071,370	10,905,560	1.5%
	November	8,489,080	8,250,323	2.9%
	Total	140,981,460	138,339,577	1.9%

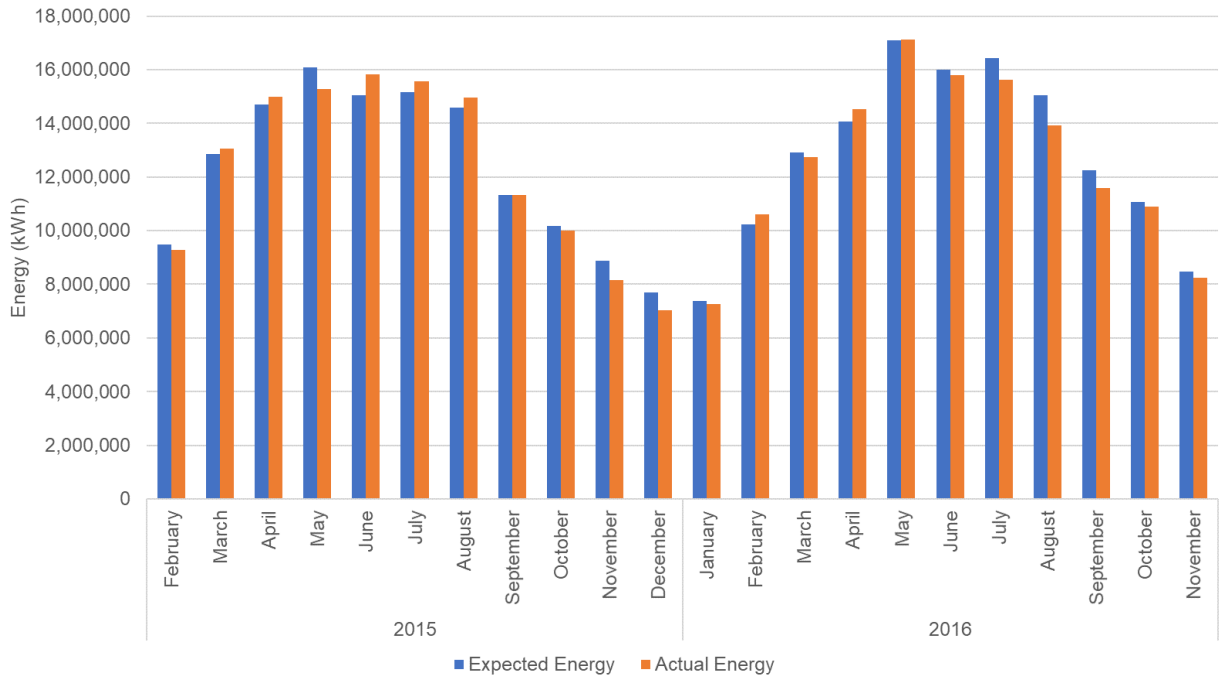

Figure 2: Comparison of Monthly Expected Energy and Adjusted Actual Energy for the Southwest PV Plant from 2015-2016.

Table 4 and Figure 3 show the Monthly Expected Energy compared with the Monthly Adjusted Actual Energy for the Southeast plant. For each month of 2017, as well as the

overall year, the Southeast plant SAM model had <10% discrepancy with actual plant data.

Table 4: Comparison of Plant-Level Monthly Expected Energy and Adjusted Actual Energy for the Southeast Plant in 2017.

Month	Monthly Expected Energy (kWh)	Monthly Adjusted Actual Energy (kWh)	Percent Difference (%)
January	97,039	103,404	-6.2%
February	108,681	108,524	0.1%
March	138,224	146,119	-5.4%
April	140,589	144,738	-2.9%
May	148,329	156,519	-5.2%
June	132,685	138,741	-4.4%
July	155,020	159,645	-2.9%
August	129,053	138,144	-6.6%
September	144,019	137,307	4.9%
October	127,666	133,259	-4.2%
November	103,800	107,820	-3.7%
December	75,901	80,634	-5.9%
Total	1,501,005	1,554,855	-3.5%

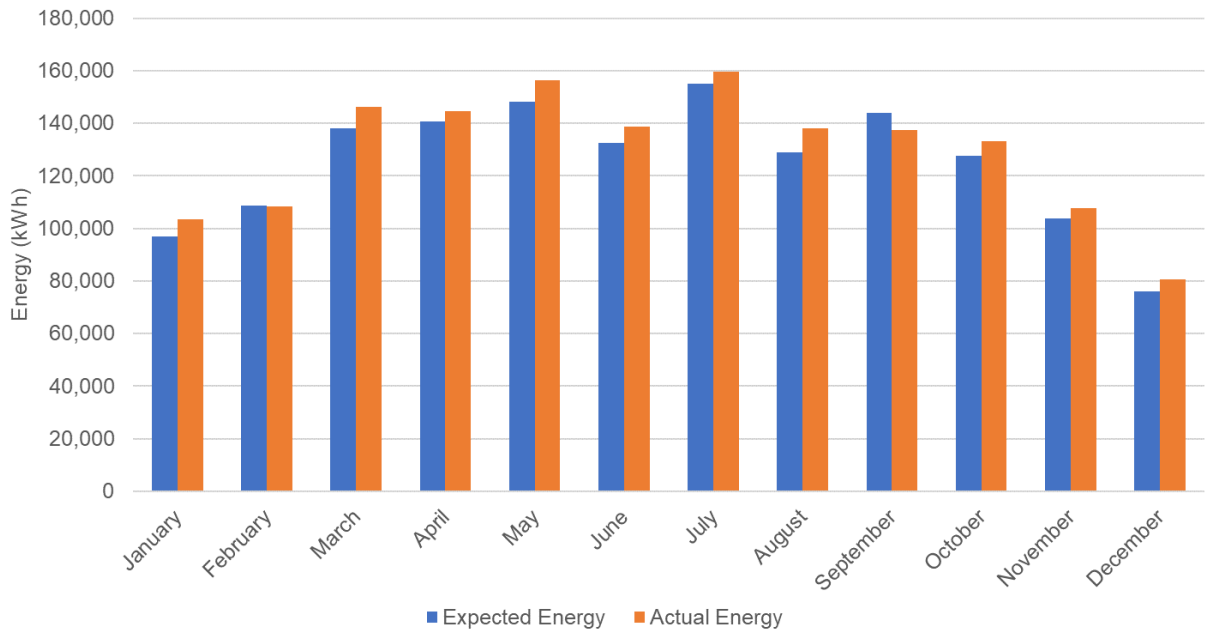

Figure 3: Comparison of Monthly Expected Energy and Adjusted Actual Energy for the Southeast PV Plant in 2017.

Data available for the Midwest location had limited plant array and module stringing information as well as limited inverter-level performance data. Therefore, inverter- and array-level analysis was not performed for detailed calibration as was done with the Southwest and Southeast plants prior to the plant-level model analysis. Instead, a plant-

level model was developed and directly compared to available, recorded plant performance data (see Table 5 and Figure 4). The majority of months for the Midwest plant model had Monthly Expected Energy that was within 10% of the Monthly Adjusted Actual Energy from actual plant data. However, there were months with greater than 10% discrepancy between modeled expected energy and actual plant data. These discrepancies are due to documented issues, including plant vegetation overgrowth causing shading in August 2016 and major snow events in December 2016 and January 2017, and are therefore not deemed to be indicative of model error.

Table 5: Comparison of Monthly Expected Energy and Adjusted Actual Energy for the Midwest Plant from 2016-2017.

	Month	Monthly Expected Energy (kWh)	Monthly Adjusted Actual Energy (kWh)	Percent Difference (%)
2016	May	392,898	395,029	-0.5%
	June	450,480	483,360	-6.8%
	July	407,182	442,541	-8.0%
	August	391,461	343,793	13.9%
	September	373,551	390,476	-4.3%
	October	335,934	338,388	-0.7%
	November	274,027	268,104	2.2%
	December	162,712	131,539	23.7%
	Total	2,788,245	2,793,230	-0.2%
2017	January	144,773	99,400	45.6%
	February	271,324	250,554	8.0%
	March	336,126	334,897	0.3%
	April	354,835	370,895	-4.3%
	May	405,542	417,269	-2.8%
	June	455,559	459,171	-0.8%
	Total	1,968,021	1,932,186	1.9%

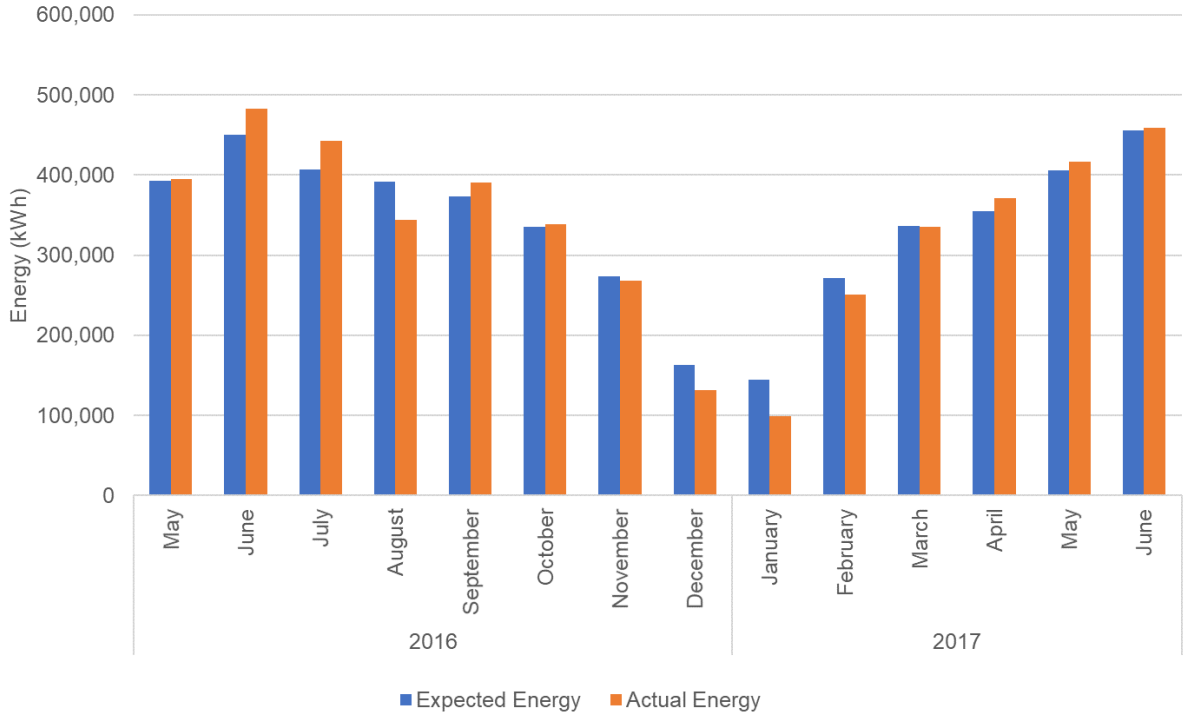

Figure 4: Comparison of Monthly Expected Energy and Adjusted Actual Energy for the Midwest PV Plant from 2016-2017.

PV Plant Economic Baseline

Following the development and calibration of the baseline models in SAM, the modeled economic performance of the three plants using SAM was compared to real plant data. While the ultimate goal of this project's analysis was to compare and optimize the LCOE of the new technologies and plant configurations explored, as a first step, economic performance was analyzed based on comparative power purchase agreement (PPA) prices. This is due to a lack of available plant-specific cost data for the plants analyzed, both on a capital cost and LCOE basis. Therefore, representative PPA prices for PV plants of a similar vintage and location as the baseline plants were identified from BloombergNEF's (BNEF's) PPA database, and capital and O&M costs based on historic EPRI cost and performance reports were used to verify baseline economic performance.

The first step in this effort was to identify PPA prices to use for comparison to SAM financial analysis results. BNEF's PPA database was filtered both by region and plant operating date to identify plants with similar characteristics to the baseline plants. The comparison PPA prices identified for each region are shown in Table 6. The PV plant capital costs for each baseline plant were developed based on past EPRI solar cost and performance studies [16][17] aligning with the vintage of the baseline plants that include cost information for several different PV technologies, including mono- and multi-c-Si and CdTe modules with fixed-tilt and single-axis tracking (SAT), with cost breakdowns for module, balance of plant (BOP), and owner's costs, as well as O&M costs. These PV technology cases were matched to the plant characteristics of the respective baseline plants, and the resulting assumed system costs for each technology type in each region are also shown in Table 6.

Table 6: Regional PPA Price and System Cost Assumptions for Economic Performance Comparison.

	Southwest Plant		Southeast Plant		Midwest Plant
Operation Date:	2014		2016		2016
PV Technologies:	CdTe with SAT, c-Si with SAT		mono c-Si with fixed and SAT		multi c-Si, fixed
PPA Prices for Comparison:					
PPA Price (¢/kWh)	8.42		6.67		6.12
PPA price escalation:	0%		0%		2%
System Costs:					
	c-Si, SAT	CdTe, SAT	mono c-Si, fixed	mono c-Si, SAT	multi c-Si, fixed
Modules ($/Wp)	0.72	0.69	0.53	0.53	0.47
BOP ($/Wp)	1.69	2.05	1.12	1.32	1.12
Owner's Cost ($/Wp)	0.22	0.24	0.13	0.15	0.13
Total Capital Required ($/Wp)	*2.63*	*2.98*	*1.78*	*2*	*1.72*
O&M ($/kW-yr)	21.9	22.8	17.2	19	17.2

System costs were input into the baseline SAM models. For plants that had multiple technologies across multiple arrays, technology cost assumptions were matched with the array's technology.

Financial assumptions for the analysis were developed based on historical data and observed trends for PV project financing and incentives. Most financial assumptions were consistent across all three plants, with the exception of internal rate of return (IRR) target, which was assumed to be higher for the 2014-vintage Southwest plant than the 2016-vintage Southeast and Midwest plants based on the assumed increased risk associated with earlier plants and trends captured by the NREL [18][19], and PPA escalation assumptions, which were adjusted to match the escalation rate associated with the comparison PPAs. Table 7 shows the financial assumptions for the three plants.

Table 7: Financial Assumptions for Economic Performance Comparison.

	Southwest Plant	Southeast Plant	Midwest Plant	Notes:
Financial Parameters:				
Analysis period:	25			Based on PPA life for comparison PPA
Inflation rate:	2%			In line with inflation rates seen between 2010 and 2016
Real discount rate:	5%			Slightly lower than WACC, achieves positive NPV
Federal income tax rate:	35%			Supported by past EPRI assumptions and NREL [16][17][18]

State income tax rate:	6%			Supported by past EPRI assumptions and NREL [16][17][18]
Debt %:	40%			Supported by NREL [18]
Tenor:	15			Typical EPRI assumption
Annual interest rate:	5%			Supported by NREL [18]
Revenue:				
IRR Target:	9.0%	7.5%	7.5%	Supported by NREL [18][19]; assume a higher expected IRR for 2014 compared to 2016 plants
IRR Year:	25			Full term of PPAs
PPA price escalation:	0%	0%	2%	Based on escalation rate assumed for comparison PPAs
Incentives:				
Investment Tax Credit:	30%			Available ITC at the time of project construction and start
Depreciation:				
MACRS:	5 years			Baseline assumption for solar PV plants

After defining the plant costs and their associated financial assumptions, each plant model was run in SAM to evaluate the associated first-year PPA. For plants that consisted of multiple arrays and multiple technologies, a generation-weighted average was used to develop the full plant's PPA. The total plant PPA was then compared with the PPAs identified for each plant to verify if the modeled plant economics produced reasonable results. Analyses were conducted for each plant using both the customized weather files developed based on plant POA data and the PSMv3 weather files for a typical meteorological year (TMY). While the files based on plant data represent a specific year of plant operation, it is expected that any financial analysis done for a plant would use a TMY dataset to understand the averages that might occur over the lifetime of the plant. Table 8 shows the assessment of the modeled Year 1 PPA price versus the comparison PPA price for each location for each of the two weather file analyses. While the TMY cases were typically closer to the comparison PPA price, all cases were within the +/-25% milestone goal laid out for this analysis.

Table 8: Modeled Year 1 PPA Price vs. Comparison PPA Price.

	Southwest Plant		**Southeast Plant**		**Midwest Plant**	
Weather File	TMY	Plant Data	TMY	Plant Data	TMY	Plant Data
Modeled First Year Output (MWh)	148,124	147,619	1,589	1,480	4,482	3,871

Modeled Year 1 PPA Price (¢/kWh)	8.33	8.37	7.59	8.15	6.43	7.46
Comparison PPA Price (¢/kWh)	8.42	8.42	6.67	6.67	6.12	6.12
Difference	-1%	-1%	14%	22%	5%	22%

PV Plant Baseline Adjustments and Updates

After calibrating the baseline SAM models, the performance and cost metrics for modules and inverters, system losses, and financial parameters were updated to match current manufacturer specifications and plant configurations to better compare modern PV technologies with the novel PV technologies investigated. These updated models served as the baseline for the remainder of the study.

Table 9 shows the technology and modeling assumptions used for the updated baseline models.

Table 10 shows the updated system costs assumed and Table 11 shows the updated financial assumptions. Finally, Table 12 shows the resulting first year annual energy output and resulting LCOE for these updated models, which served as the baseline for comparison with future technologies.

Table 9: Updated 2020 Baseline Model Assumptions/Methodology.

	Southwest Plant	Southeast Plant	Midwest Plant
Modules	First Solar Series 6 (445W); LONGi Solar, mono c-Si (385 W)*	LONGi Solar, mono c-Si (385 W)*	LONGi Solar, mono c-Si (385 W)*
Racking Height	No change		
Orientation and Tracking	No change		
System Design	DC capacity held as constant as possible given module/inverter changes. Grid limits applied to match baseline AC capacity, where appropriate; DC and AC losses adjusted to reflect component losses*		
Inverter Design	Updated to SMA Sunny Central 2500-EV-US* inverter operating at 1,500V; Number of inverters adjusted to achieve similar DC:AC ratio to baseline model	No change to inverter specifications* or number of inverters	Updated to Sungrow SG250HX* inverter operating at 1,500V
Module Stringing	Modules per string adjusted due to changes in module voltage and/or inverter MPPT requirements; Strings in parallel adjusted to keep DC capacity as constant as possible, while also maintaining similar row self-shading layout (see below).		

Row Self-Shading	Modules along row kept constant; Modules at bottom of row varied to achieve a whole number of rows, when possible
Total Plant Area	No change to ground coverage ratio; Total plant area automatically adjusted based on number of modules and rows, constrained by original land area.
*Based on specifications in EPRI's 2020 solar cost and performance report [20]	

Table 10: Updated 2020 System Cost Assumptions.

	Southwest Plant		Southeast Plant		Midwest Plant
System Costs:					
	c-Si, SAT	CdTe, SAT	mono c-Si, fixed	mono c-Si, SAT	multi c-Si, fixed
Modules ($/Wp)	0.33	0.28	0.33	0.33	0.33
BOP ($/Wp)	0.47	0.47	0.38	0.47	0.41
Indirect Costs ($/Wp)	0.18	0.17	0.16	0.17	0.16
Total Capital Required ($/Wp)	*0.97*	*0.92*	*0.87*	*0.97*	*0.90*
O&M ($/kW-yr)	13.7	13.5	12.1	13.7	12.1

Table 11: Updated 2020 Financial Assumptions for Economic Performance Comparison.

	All Plants	Notes:
Financial Parameters:		
Analysis period:	25	Consistent with original
Inflation rate:	2%	Consistent with original
Real discount rate:	5%	Consistent with original
Federal income tax rate:	21%	Updated based on EPRI assumptions for current projects
State income tax rate:	6%	Consistent with original, varies by state
Debt %:	60%	Updated based on EPRI assumptions for current projects
Tenor:	15	Consistent with original
Annual interest rate:	5%	Consistent with original
Revenue:		
IRR Target:	7.5%	Based on original, made consistent across cases
IRR Year:	25	Full term of PPAs
PPA price escalation:	2%	Based on original, made consistent across cases
Incentives:		
Investment Tax Credit:	10%	Assumed ITC available for future PV plants

Depreciation:		
MACRS:	5 years	Consistent with original

Table 12: Updated 2020 Baseline Model Output and LCOE.

	Southwest Plant	**Southeast Plant**	**Midwest Plant**
First Year Annual Energy Production (MWh)	145,696	1,598	4,313
Nominal Plant LCOE (¢/kWh)	3.63	5.10	5.80

Milestone Accomplishments

Milestone 1.1: Modeled power production <10% discrepancy was achieved through this effort for the Southwest and Southeast plants on both a monthly and annual basis. For the Midwest plant, the majority of months and the annual results met the <10% criteria, though there were months with greater than 10% discrepancy between modeled expected energy and actual plant data. These discrepancies are due to documented issues, including plant vegetation overgrowth causing shading in August 2016 and major snow events in December 2016 and January 2017, and are therefore not deemed to be indicative of model error.

Milestone 1.2: Modeled plant economics <25% discrepancy was achieved through the baseline plant economic analysis, with the models using TMY weather files achieving a modeled first-year PPA price within 14% of comparison prices, and those using a specific year of plant-procured weather data, which is less likely to be used for a plant's lifetime economic analysis, coming within 22% of the comparison price.

Task 2: Technology Cost and Performance Discovery

A comprehensive literature review was conducted to identify background information for the technologies analyzed in this project. Over sixty technical reports, articles, and web documents were reviewed to capture the characteristics and the current state of bifacial modules, tandem modules, 1500V+ plant architectures, and module-level power electronics (MLPE). Insights around bifacial modules included the trade-off between increased performance/heat dissipation with increased bifacial module array height versus increased racking costs, with performance saturation estimated at array heights above 2 meters [2][21][22]. Additional literature insights, such as a methodology for modeling low-cost, 4T perovskite-silicon tandem modules, potential benefits of microinverters over string inverters, and challenges associated with increasing plant voltages to greater than 1500V_{DC}, were collected [10][23][12]. Insights from this review were collected and incorporated into modeling assumptions and strategy.

Informational interviews were also conducted to collect detailed information on the technologies analyzed in this project. More than a dozen industry experts including researchers, equipment and module manufacturers, and engineering firms were contacted with detailed questionnaires pertaining to characteristics of the technologies analyzed. Bifacial module technical datasheets were acquired from PV manufacturers,

providing the parameters required to capture the performance of these state-of-the-art modules more accurately. Tandem module specifications obtained during these interviews helped to inform and confirm the modeling methodology used. The informational interviews also resulted in an improved understanding of increased voltage architectures and capabilities, with responses from interviewees indicating that current components and equipment can likely handle increased voltages (1500V+), but that current electrical code requirements, not component/equipment capability, would be the greatest limiting factor for adoption of increased voltages within the next five years. Insights and responses from these interviews were used to inform the incorporation of the new PV technologies into SAM. As the project progressed, additional outreach to and conversations with solar contractors, developers, and technology experts further informed technology and cost assumptions around future technologies that are currently not on the market. In total, 20 experts from 14 companies provided input to the project. While many requested that their responses be anonymized due to the speculative nature of the conversations, the insights that were provided significantly helped inform project assumptions.

Milestone Accomplishments

Milestone 2.1: >40 technical papers reviewed and Milestone 2.2: >16 informational interviews conducted were both achieved through the Technology Cost and Performance Discovery task, with over sixty technical reports, articles, and web documents reviewed and summarized and conversations with twenty experts used to inform the assumptions and analysis.

Task 3: PV Plant Modeling Optimization

Parameters for each of the technologies analyzed were incorporated into SAM to understand their impacts on plant performance and which design parameters most influenced plant output. New technology costs and equipment-level adjustments between the baseline models and the new technology cases were then incorporated into the model and, when applicable, evaluated using an optimization algorithm to understand the trade-offs between different plant design options and technical specifications to achieve the lowest plant LCOE.

PV Plant Performance Modeling

Bifacial Modules

Two custom bifacial modules were created within SAM, based on datasheets provided during the informational interview process, and incorporated into the SAM models for each plant utilizing hourly albedo values within the weather files for bifacial gain calculations. System design specifications, such as modules per string and strings in parallel, were adjusted to accommodate the inclusion of bifacial modules based on module performance characteristics. The remaining plant specifications, such as DC:AC ratio, plant capacity, ground coverage ratio (GCR), and module ground clearance height, were set to match those of the baseline models. These models were then simulated within SAM. These “non-optimized” models were then analyzed for bifacial module optimization sensitivities including varying ground clearance height, GCR, and albedo grooming.

Bifacial modules were first incorporated into the Southwest plant. A surprising result in the initial Southwest plant simulations with bifacial modules was a *decrease* in plant output compared to the baseline model. Further examining these results indicated that the significant decrease in plant output occurred in the plant arrays that originally used thin-film CdTe modules, with several factors leading to this result.

When bifacial c-Si modules were incorporated into the baseline plant's arrays originally composed of SAT, non-backtracking CdTe arrays, the impact of the inherent difference between CdTe and c-Si module temperature coefficients and the linear shading response of CdTe cells versus the non-linear shading response of c-Si cells was observed. To better understand these impacts, first, a comparison of CdTe and c-Si temperature coefficients was investigated, indicating that CdTe temperature coefficients can positively affect monthly plant performance by 0.2 to 1.4%, depending on location and the modules being compared. This is further discussed in Task 4. Temperature coefficients are dependent on cell technology, design, and manufacturing processes, and are not a module characteristic that can be improved upon by a plant developer, but the results helped to partially explain the initial results.

Module shading response, which is also intrinsic to each module's cell technology and cell orientation, was also a suspected culprit in the lower performance of the bifacial plant. The First Solar Series 6 CdTe modules used in this analysis are designed such that each cell spans the entire length of the module. As a result, when a module experiences row-to-row shading, cells are shaded equally when mounted in a portrait configuration, as recommended by First Solar. In comparison, c-Si cells, like those in the bifacial modules, do not span the entire length of the module, resulting in unequal shading of c-Si cells when row-to-row shading occurs. This non-linear shading effect of c-Si cells negatively affected plant performance of bifacial c-Si modules upon initial incorporation into the Southwest plant. This is further discussed in Task 4. However, these effects can be mitigated by the addition of backtracking where row-to-row shading is avoided through a tracking algorithm, a feature typical within the industry for monofacial and bifacial c-Si modules. Adding backtracking into the Southwest plant resulted in an 8.8% gain in overall energy compared to the non-backtracking case and a 1.1%-2.3% gain in overall energy output compared to the baseline.

Additional sensitivities looking at adjustments to system design such as GCR and minimum ground clearance height also showed improvement in plant output for the Southwest plant.

GCR is defined as the ratio between the module area and the PV plant land area, which can be simplified as the collector width of an array over the row-to-row distance. As GCR decreases, row-to-row distance increases and as GCR approaches 1.0, row-to-row distance decreases. This ratio is used to calculate row-to-row shading for an array, as well as to calculate the total land area of the plant. To analyze the effects of row spacing on PV plant performance, GCR was adjusted compared to baseline plant designs. Because the power density of the plant increased by replacing the baseline CdTe and monofacial c-Si modules with the bifacial modules' increased rated output power, initial incorporation of bifacial modules with the same GCR as the baseline led to 13.5% less required land for the same power output. Increasing the GCR to match the original available land area allowed for improved row-to-row spacing, leading to increased

reflected sunlight to the backside of bifacial modules. As investigated further in the economic and optimization analysis, it also impacts the total land area of the plant, which impacts system costs.

Furthermore, a sensitivity was conducted to look at raising the ground clearance to 5 meters. Literature insights discuss the trade-off between increased performance with bifacial module arrays versus increased racking costs for heights above approximately 2 meters [2][21][22]. Typically, as the ground clearance height of bifacial modules increases, reflected light to the backside of each module is also increased, positively affecting energy yield overall. However, the limit of this performance gain can be site-specific, and heavily affected by costs. To capture the potential performance effects associated with increased ground clearance height, the performance impact of an extreme case of 5 meters was analyzed, showing additional improvement of reflected sunlight to the backside of bifacial modules. However, as with GCR, this also impacts plant cost, and tradeoffs between cost and performance were investigated further in the economic and optimization analysis. Performance results for the Southwest plant sensitivities are shown in Figure 5.

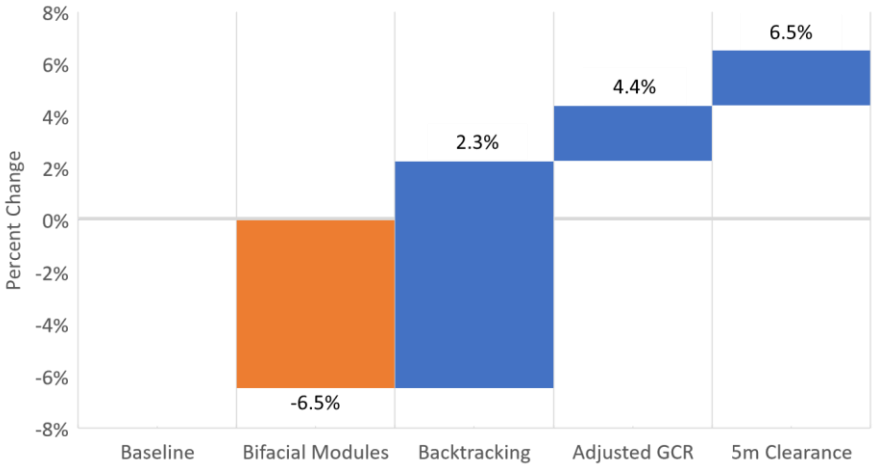

Figure 5: Bifacial Module Energy Gain/Loss for Optimization Sensitivities for the Southwest Plant.

Similar methodology and analyses were performed for the Southeast and Midwest plants, excluding the addition of backtracking technology. The Southeast plant employs mostly fixed-tilt arrays with one SAT, backtracking array. Therefore, backtracking was already captured where applicable for incorporation of bifacial c-Si modules. The Midwest plant is an entirely fixed-axis array and, therefore, has no need for backtracking. Southeast and Midwest bifacial sensitivity results are shown in Figure 6 and Figure 7. These models' performance versus cost were later captured via parametric analyses and optimization algorithm.

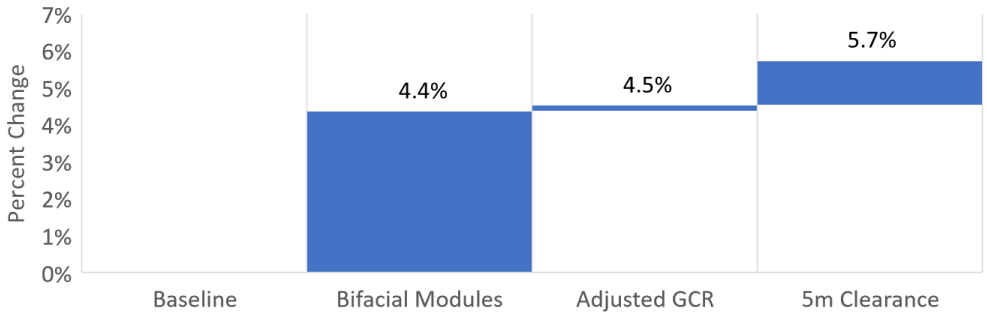

Figure 6: Bifacial Module Energy Gain for Optimization Sensitivities for the Southeast Plant.

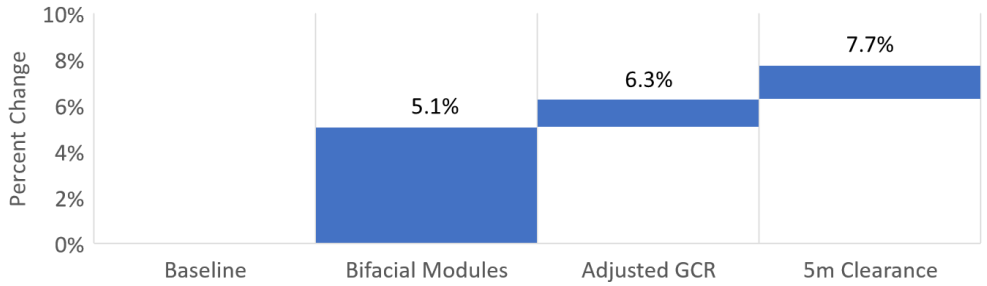

Figure 7: Bifacial Module Energy Gain for Optimization Sensitivities for the Midwest Plant.

Tandem Modules

A custom 4T perovskite-silicon tandem module was developed within SAM based on industry literature, existing module specifications, and informational interview responses. 4T tandem modules allow for a mechanical stacking approach to developing a utility-scale tandem module within SAM, while two-terminal (2T) tandem modules require voltage or current matching between each tandem layer, which is difficult to model given SAM's custom module input limitations. For this reason, a mechanically stacked 4T tandem module was developed for investigation. This 4T configuration would result in two different stringing voltages associated with the top layer and bottom layer, which SAM's system design, inverter specifications, and cost parameters are not designed to capture. To solve this stringing complexity, this analysis assumes module-level power electronics that would be able to combine these two voltages, yielding 2T output for a 4T tandem module that can be strung back to the inverter. These module-level power electronics are typically a fraction of a cent for tandem modules and are assumed negligible in cost relative to the cost of tandem modules.

To establish the framework for a custom monofacial 4T utility-scale tandem module, specifications from the baseline c-Si module (LONGi Solar's LR6-72HPH-385M) were utilized. The monofacial 4T tandem module efficiency of 26.5% reported by Coletti et al. (2020) [9] was then referenced to establish a scale factor between the baseline module and a tandem module. This scale factor was applied to each of the baseline module's specifications, with the temperature coefficient of V_{oc} assumed to receive the full benefit of the tandem structure and temperature coefficient of I_{sc} remaining constant. All other module specifications were scaled equally. The resulting specifications are listed in Appendix A.

This custom tandem module was then incorporated into each plant model within SAM. System design specifications, such as modules per string and strings in parallel, were adjusted to accommodate the inclusion of tandem modules based on module performance characteristics. The remaining plant specifications, such as DC:AC ratio, plant capacity, and GCR, were set to match those of the baseline models. Due to their increased power density and efficiency, initial incorporation of tandem modules into a plant utilizing the same GCR as the baseline leads to significantly less required land area. This is particularly true for the larger Southwest plant.

To understand the boundaries of tandem module performance optimization, two sensitivities were included for the Southwest plant – adjusted GCR and adjusted DC capacity. Adjusting the GCR to utilize the original available plant land area resulted in increased overall performance due to less row-to-row shading of modules. To adjust the overall DC capacity, additional tandem modules and inverters were added to maintain a similar DC:AC ratio as the baseline, utilizing the full available plant area with the same GCR as the baseline, increasing the capacity and overall energy output of the Southwest plant. The monthly energy output for the Southwest plant under these sensitivities is shown in Figure 8. Similar but scaled effects are expected for the Southeast and Midwest plants, but were not modeled in the initial technology incorporation. Monthly energy output of the Southeast and Midwest plants with tandem modules utilizing the same GCR and DC plant capacity as the baseline are shown in Figure 9 and Figure 10.

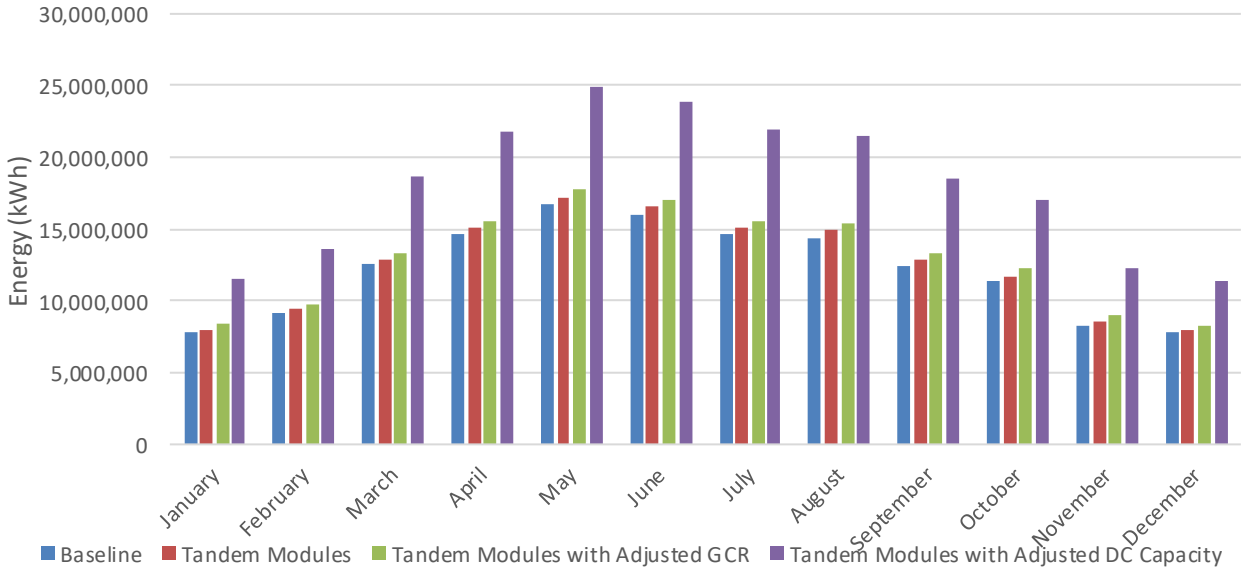

Figure 8: Monthly Energy of Tandem Modules and Tandem Module Optimization Sensitivities for the Southwest Plant.

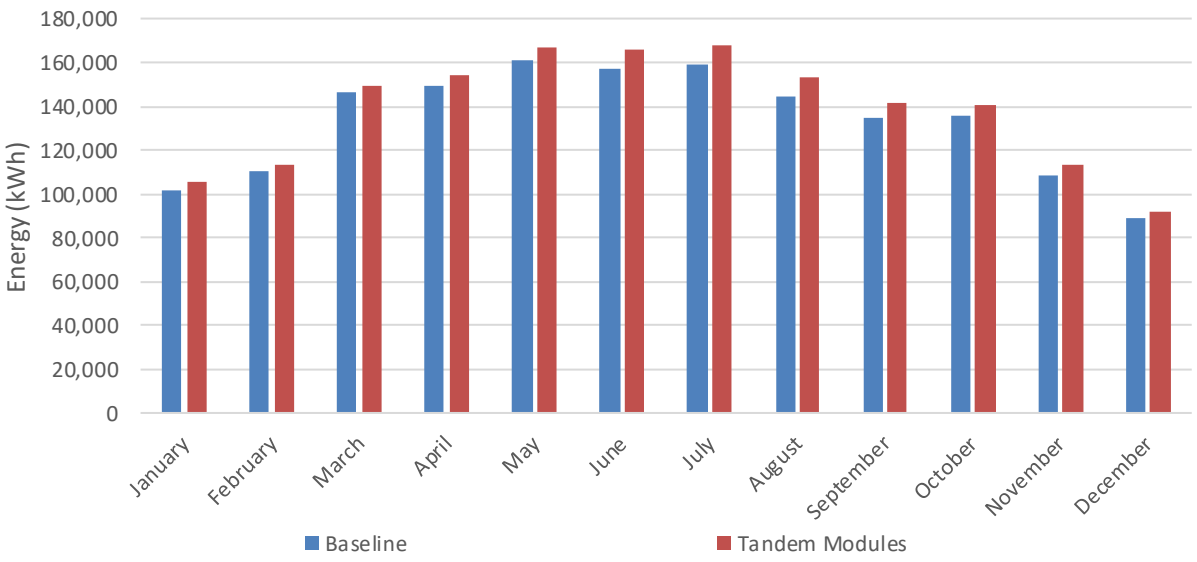

Figure 9: Monthly Energy of Tandem Modules for the Southeast Plant.

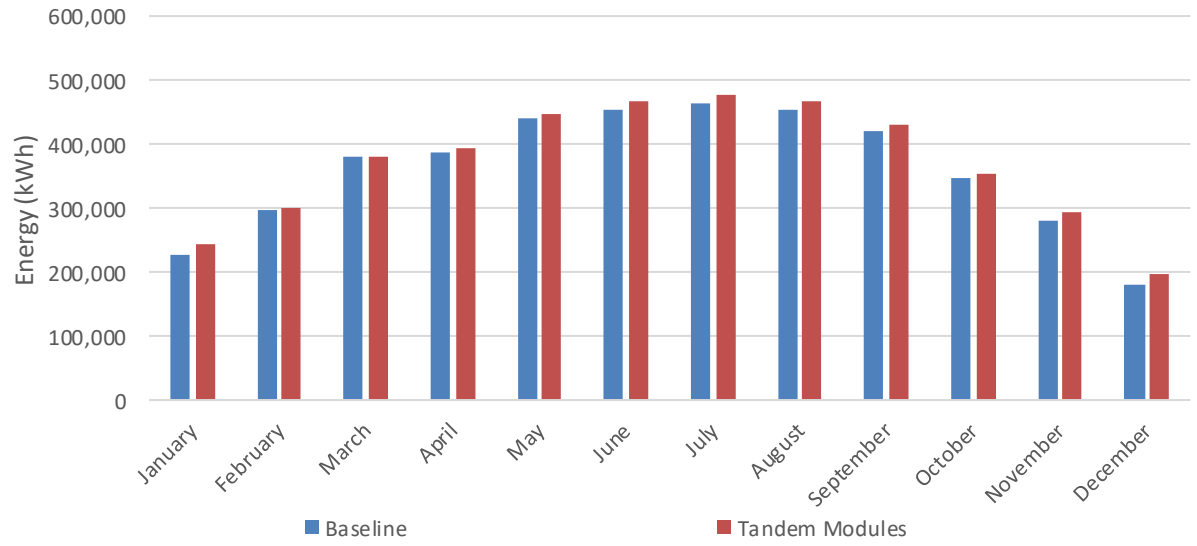

Figure 10: Monthly Energy of Tandem Modules for the Midwest Plant.

This analysis shows the inherent performance gain from incorporation of tandem modules in all three plants due to their greater efficiencies and power density compared to the baseline modules. However, there will ultimately be a LCOE trade-off between module cost, plant performance, total land area, and other parameters. The economic viability of using tandem modules and adjusting GCR or plant capacity were later analyzed via economic modeling and optimization analysis.

Increased Plant Voltages

Plant architectures of 2000V, 2500V, and 3000V were investigated to understand the impact over a range of increasing voltages. This analysis focused primarily on the inverters required to operate a PV plant at these higher voltages. Through the

informational interview process, industry experts indicated that codes and standards would likely be a key hurdle for increasing plant voltages above 1500V, which is currently the maximum that the National Electric Code (NEC) allows. Many components would likely be more expensive to account for increased insulation thicknesses and more skilled labor needs for installation, but this analysis assumed that all other plant components beyond the inverters could handle increased voltages without significant changes beyond cost.

Because there are currently no inverters in the market designed to operate at these increased voltages, custom inverters needed be developed to conduct this analysis. This required several assumptions to be made around the relationship between inverter voltage and maximum inverter rating, maximum DC current, inverter efficiency, and minimum and maximum power point tracking (MPPT) voltages, all of which impact the design and performance of a PV plant.

To estimate the new characteristics for these inverters, 90+ inverter datasheets from five different manufacturers were compiled to serve as data points to inform the inverter specifications of the custom 2000V, 2500V, and 3000V inverters. These data points were sorted by maximum DC voltage and plotted as their maximum AC power output versus maximum DC current (see Figure 11). This scatter plot allowed for linear regressions to be calculated for each existing inverter voltage at 600V, 1000V, and 1500V. Utilizing a scale factor between the slopes of those regression lines, new regression lines for 2000V, 2500V, and 3000V inverters were calculated. From there, two approaches were considered for developing inverter assumptions: one assuming the same AC power output of the baseline inverters and one assuming the same DC current as the baseline inverters. Using the regression lines, this can be used to solve for the DC current or maximum AC power output of each plant's 2000V, 2500V, and 3000V inverters. In addition, subject matter experts were interviewed to provide insights and new assumptions to approximate future inverter specifications. These discussions indicated that the more likely assumption is that the maximum AC power output of these inverters would increase as the voltage increases. Therefore, the remaining analysis assumed that the DC current for the inverters remained the same and the maximum AC power increased.

To calculate other inverter specifications, inverter AC voltages were scaled using the ratio between baseline AC voltages and baseline maximum DC voltages to calculate the AC voltages of the 2000V, 2500V, and 3000V custom inverters. Next, the ratio between the baseline AC voltages and minimum MPPT voltages were applied to the custom inverter AC voltages to define the custom inverter minimum MPPT voltage. These calculated inverter specifications for the Southwest, Southeast, and Midwest plants at each voltage level are listed in Appendix A.

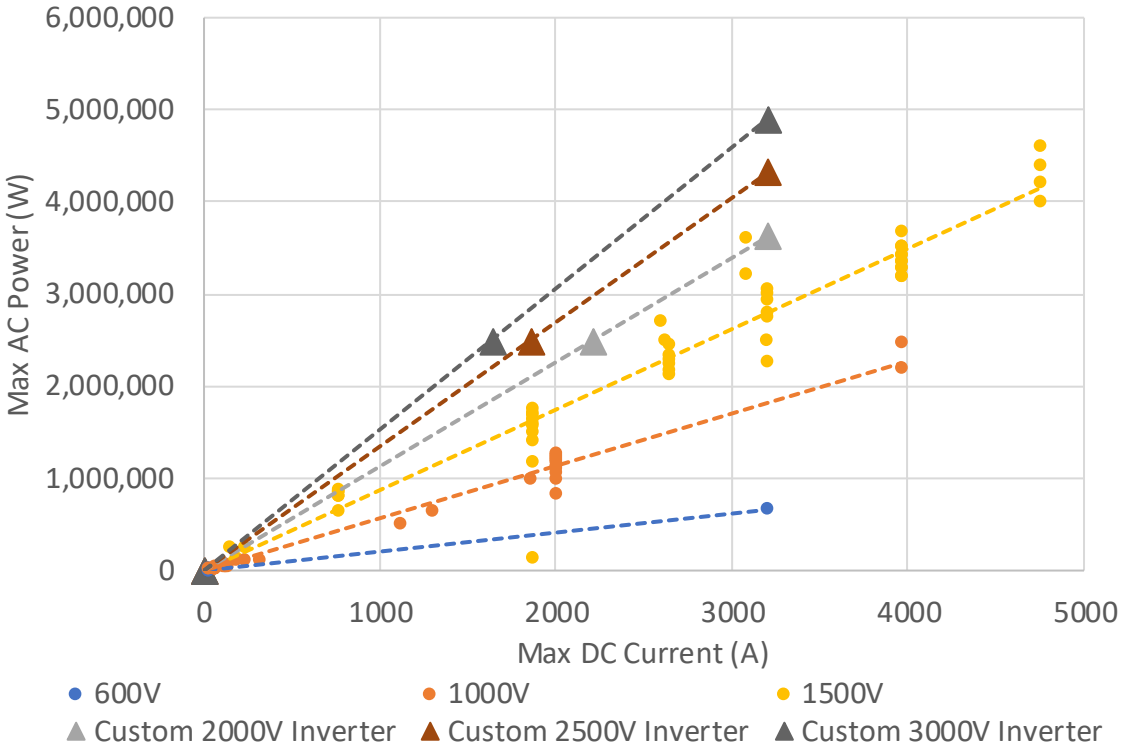

Figure 11: Relationship Between the Max DC Current and Max AC Output Power for Existing 600V, 1000V, and 1500V Inverters and Custom 2000V, 2500V, and 3000V Inverters

To model plant performance, DC and AC system losses were adjusted to capture decreased wiring losses due to increased system voltages. Utilizing a voltage drop calculator, DC system losses for the 2000V, 2500V, and 3000V cases were estimated. The percent change in voltage drop for DC losses were also utilized to estimate AC losses for each voltage step. Assumptions for DC and AC system losses are shown in Table 13.

Table 13: DC and AC System Loss Assumptions for Increased Voltage Architectures.

PV Plant	DC Losses				AC Losses			
	Base	2000V	2500V	3000V	Base	2000V	2500V	3000V
Southwest Plant	1%	0.65%	0.5%	0.4%	0.75%	0.5%	0.4%	0.3%
Southeast/ Midwest Plants	0.6%	0.4%	0.3%	0.25%	1%	0.6%	0.5%	0.4%

As the new higher-voltage, higher-capacity inverters were incorporated into SAM, a challenge arose that for some of the smaller plants the size of a single inverter began to be larger than the DC rating of the array it is tied to. To accommodate this, system DC capacity was adjusted to maintain similar DC:AC ratios for each array, despite increased AC capacity due to increased DC voltage. Figure 12, Figure 13, and Figure 14 show the resulting monthly capacity factors of the increased plant voltages. Note, plant capacity factors are shown rather than annual energy production due to the adjustments made in AC capacity to maintain DC:AC ratios for each array, which would make comparing energy output inconsistent.

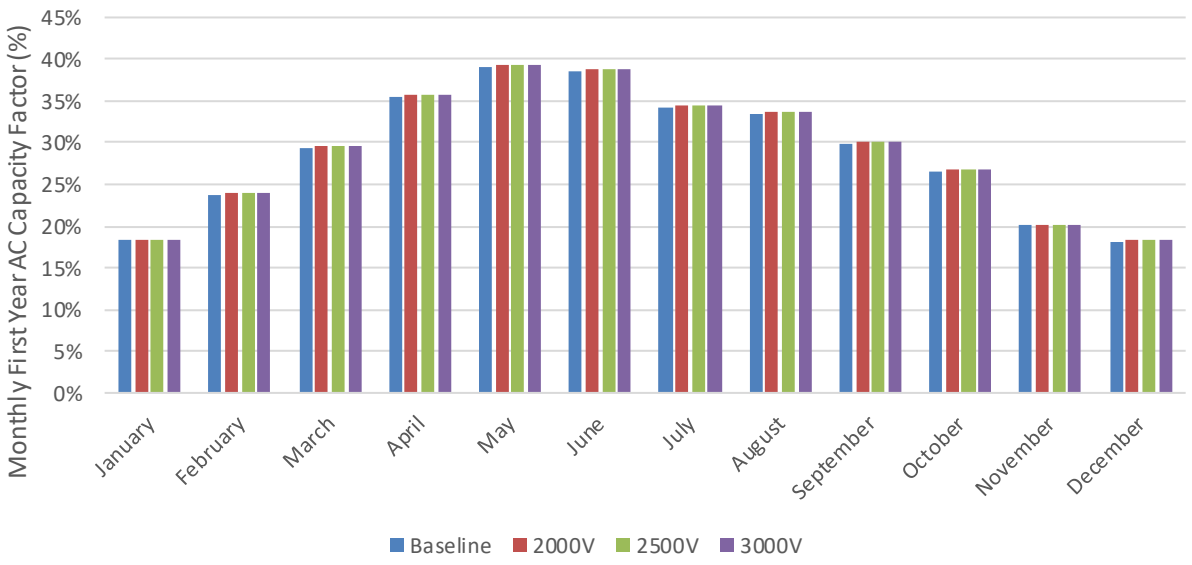

Figure 12: Monthly Capacity Factor for Increased Voltage Architectures for the Southwest Plant.

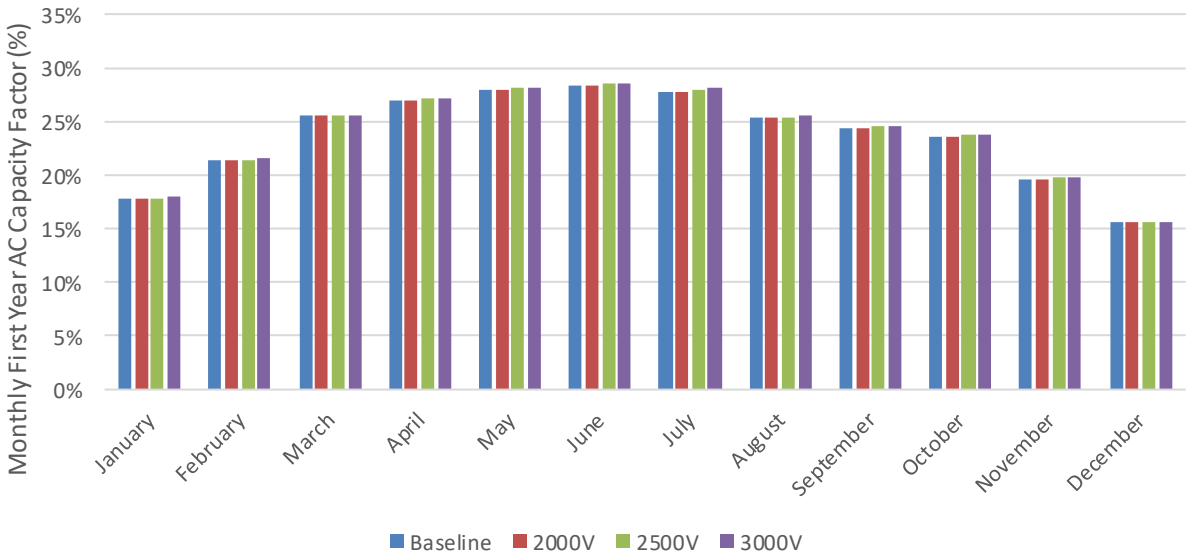

Figure 13: Monthly Capacity Factor for Increased Voltage Architectures for the Southeast Plant.

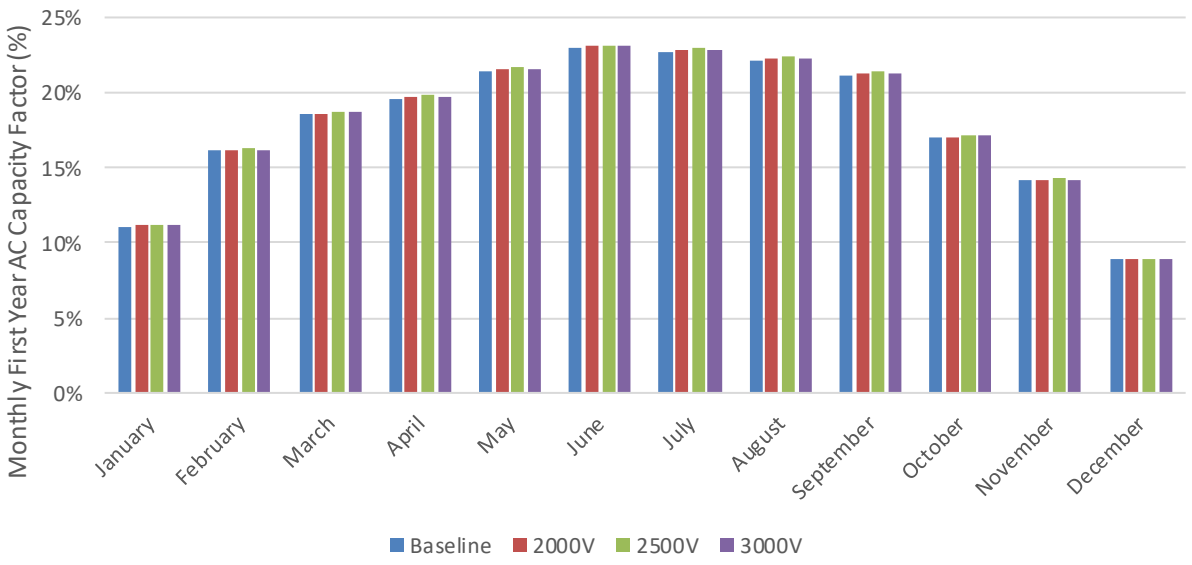

Figure 14: Monthly Capacity Factor for Increased Voltage Architectures for the Midwest Plant.

In many cases, overall plant performance and energy output is relatively unchanged as plant voltage architecture increases, with small increases in plant capacity factor driven primarily by the decreased system losses assumed. Instead, industry motivation for increasing plant voltage architectures has typically been centered around reduction of capital costs and, as a result LCOE, due to fewer required strings and associated costs rather than direct plant performance improvements. This was investigated through the economic analysis.

Module-Level Power Electronics

Two different MLPE technologies were considered for this analysis: microinverters and DC-DC optimizers.

For the microinverter analysis, Enphase's IQ7A microinverter was used as a reference to develop a custom inverter to act as each plant's microinverter (see Appendix A). By definition, module-level power electronics are applied to each module. Therefore, to apply a microinverter to each module, the number of inverters, strings in parallel, and modules per string were adjusted within each model to simulate one microinverter per module. Next, module mismatch assumptions were adjusted to account for microinverter performance. Typical PV plant module stringing design strings multiple modules together and the string or central inverter performs Maximum Power Point Tracking (MPPT) on the voltages associated with multiple modules. This can lead to module mismatch in cases where there are differences between the voltages of adjacent modules within the same stringing configuration. Microinverters are able to eliminate module mismatch by performing MPPT and converting each module's DC energy into AC energy at the module level. Therefore, module mismatch was changed from 0.8% to 0% for microinverter cases. These cases were then simulated in SAM with results shown in Figure 15, Figure 16, and Figure 17.

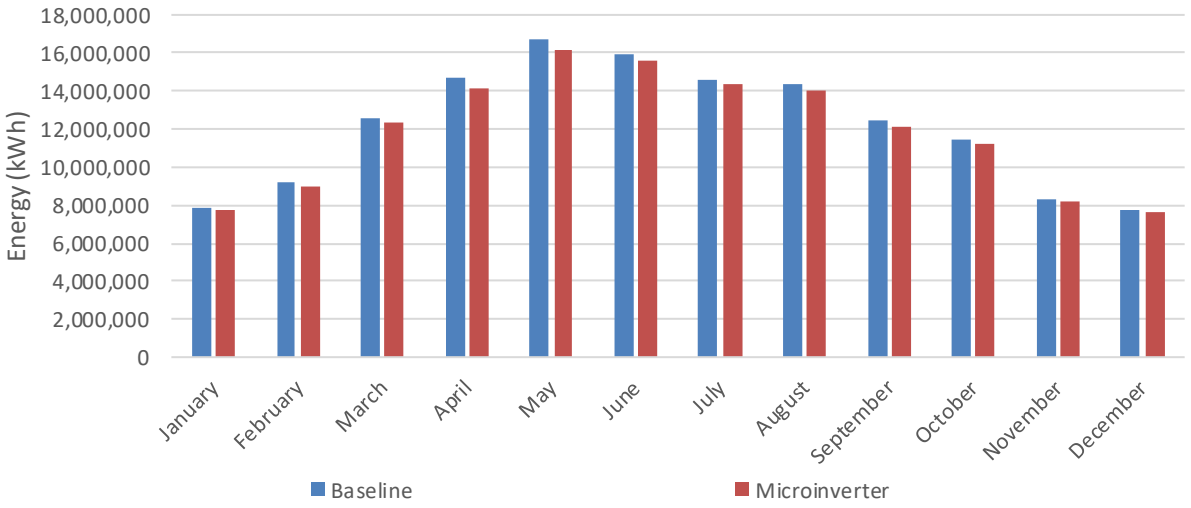

Figure 15: Monthly Energy Utilizing Microinverters for the Southwest Plant.

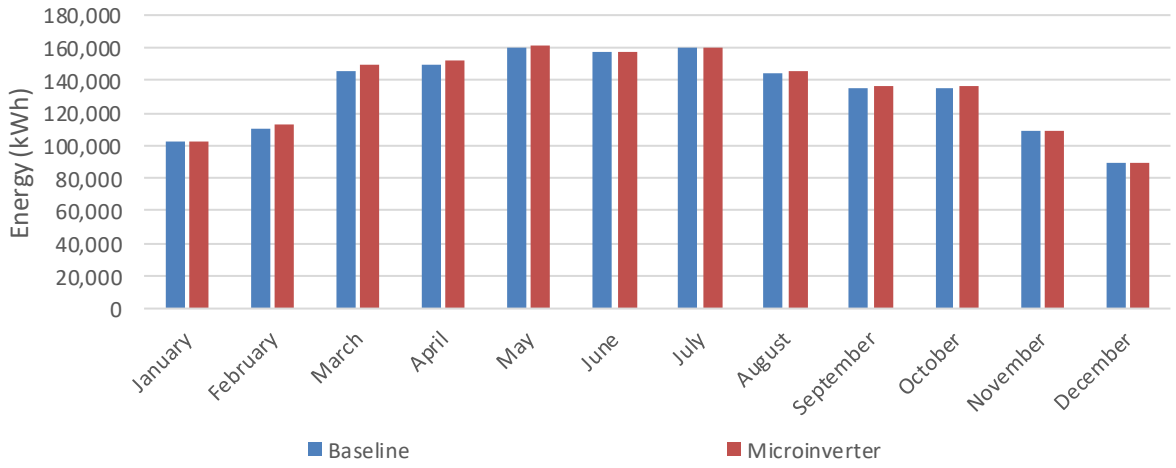

Figure 16: Monthly Energy Utilizing Microinverters for the Southeast Plant.

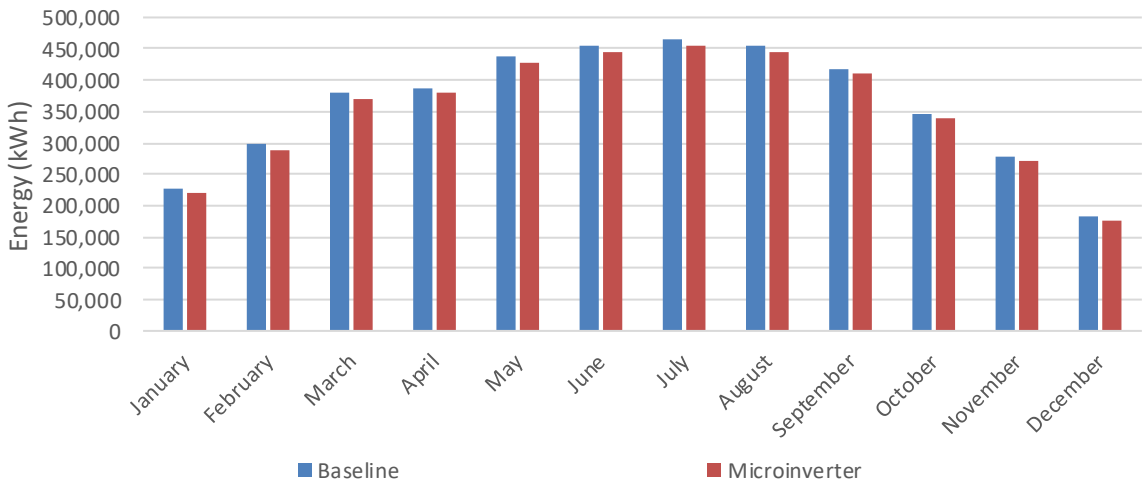

Figure 17: Monthly Energy Utilizing Microinverters for the Midwest Plant.

As shown in the results, incorporation of microinverters does not inherently guarantee increased performance outside of the elimination of module mismatch. In some cases, such as the Midwest plant, energy is lost as a result of the lower AC power rating and lower efficiency of the microinverter compared to the baseline inverter. Additionally, while microinverters are typically utilized on a residential or commercial scale to mitigate the effects of partial shading events (e.g., trees, large bushes, poles, adjacent buildings), these types of partial shading events are typically avoided or eliminated during utility-scale plant site design and preparation. Due to the utility-scale nature of the baseline models, partial shading events are not included in the model. Therefore, any benefits associated with mitigation of partial shading effects are not captured by this analysis. However, little is known about module mismatch over the lifetime of a PV plant. With degradation affecting module performance over time, module mismatch may become more dynamic than a constant loss percentage, as modeled within SAM. As a result, module mismatch loss may eventually achieve levels at some point in the plant's lifetime where the incorporation of microinverters to eliminate mismatch may be viable.

DC-DC optimizers were also investigated as part of the MLPE analysis. However, since DC-DC optimizers do not serve as inverters and are add-on components to each module that perform MPPT optimization at the module-level, SAM is limited in capturing the performance of DC-DC optimizers. As a result, DC-DC optimizer inclusion can only be captured within the module mismatch and DC power optimizer loss assumptions of the model. Changing module mismatch from 0.8% to 0% and DC Optimizer Loss to 1% (as recommended per NREL), results in a net addition of 0.2% loss overall for each plant.

PV Plant Economic Modeling and Optimization

To analyze the impact of the technologies analyzed in this study on plant economics and LCOE, the detailed cost breakdown developed for the baseline plant technologies were adjusted to incorporate new technology costs and equipment-level adjustments between the baseline models and the bifacial module, tandem module, 1500V+ plant architecture, and MLPE cases. These cost considerations and sensitivities were incorporated into SAM and, when applicable, evaluated using an optimization algorithm to understand the trade-

offs between different plant design options and technical specifications to achieve the lowest plant LCOE. The following describes the optimization algorithm selection, assumptions developed to incorporate economic costs associated with each technology, the methodology utilized to optimize technology cases, and results of each optimization and/or sensitivity analysis.

Optimization Algorithm Selection

To optimize the novel plant designs, SAM models were exported from the traditional SAM graphical interface to a Python environment, allowing for use by PySAM, a programming interface designed for reading and editing SAM/BAM/VCF/BCF files. Exporting SAM files to the PySAM environment enables the automation of many simulations with varying system parameters. Additionally, this environment makes it possible to implement custom cost equations for the novel technologies that are not yet built into SAM.

The goal when selecting an optimizer for this analysis was to find one that could achieve the minimum LCOE within a reasonable computation time. Because each PySAM model takes approximately one minute to execute, it is desirable to select an optimizer that converges efficiently. As a result, the performance of three optimizers – a traditional convergent (or gradient descent) optimizer and two evolutionary algorithms – was compared.

Traditional convergent optimizers perform well when the optimization function produces a smooth solution space. Evolutionary algorithm optimizers are inspired by biological processes and search for an optimal solution in a distributed manner using randomized parameters between iterations. These algorithms perform well with optimization functions that are non-convex as the distributed search and random mutations enable evolutionary algorithms to avoid getting stuck in local minimums.

To test and compare the different optimization algorithm options, a number of analyses were conducted to determine the tool that best balanced accuracy and computation time. These analyses were conducted on an array of the Southwest plant implementing bifacial modules, evaluating the optimization of LCOE as a function of both module ground clearance height and GCR. As a first step, a parametric sweep was conducted of the LCOE versus the ground clearance height and GCR (see Figure 18). At a high-level, the solution space appears smooth, but at a more granular level, the solution space exhibits local minimums.

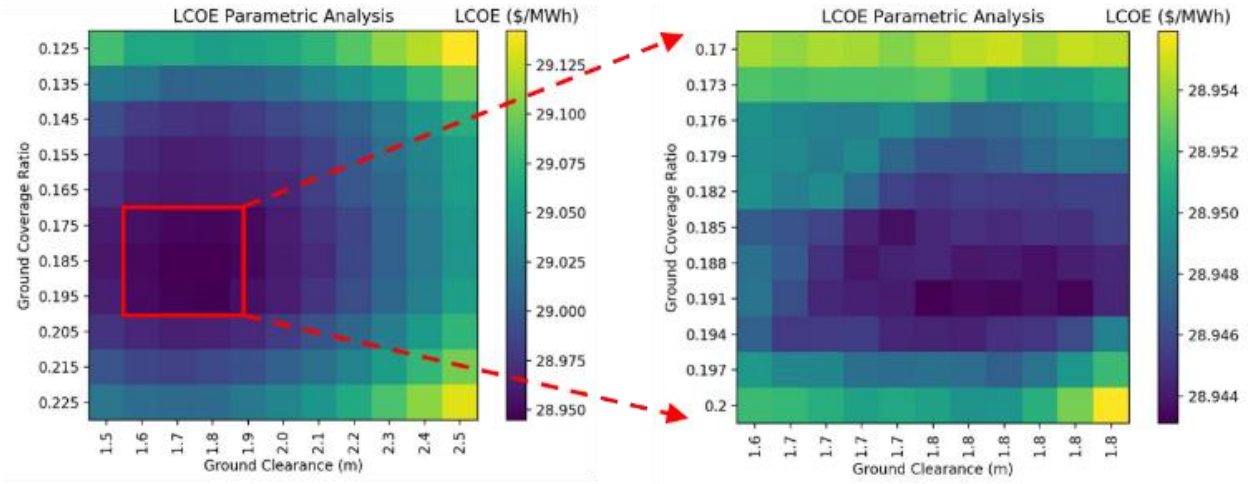

Figure 18: Parametric Sweep Results Analyzing Bifacial Module Case LCOE Versus Module Ground Clearance Height and Ground Coverage Ratio.

Two evolutionary algorithms were selected for testing: the particle swarm and the genetic algorithm. Both are well suited for numerical optimization problems. In the particle swarm algorithm, a population of individual particles navigate the parameter space. The speed and direction for each particle is governed by a combination of its locally best-known position and the global best-known position. In the genetic algorithm, there are generations of individuals with a fixed population size, constant across all generations. From one generation to the next, offspring are produced from the parent generation by mating individuals (exchanging parameters), mutating parameters, and selecting among the offspring with the highest fitness (defined as the minimum LCOE in this case). In both algorithms, a population size of 10 is selected. For implementation, the Python package Distributed Evolutionary Algorithms in Python (DEAP) was used. For the traditional optimizer, the default minimization optimizer in the Science Python (SciPy) package was used.

A challenge in the application of evolutionary algorithms is the selection of options, called hyperparameters. In each of these, there is a parameter that sets the learning rate. If the learning rate is fast, the algorithm will converge to a solution more quickly; however, there is a risk that if it is too fast it may skip over the optimal solution. A slower learning parameter takes longer to converge but has a greater chance of settling on a more optimal solution. The learning parameter for the particle swarm algorithm is the maximum velocity, whereas the learning parameter for the genetic algorithm is the mutation standard deviation. The hyperparameters were evaluated by comparing the algorithm convergence rate with a range of learning parameter values, with results shown in Figure 19 and Figure 20. The faster (larger number) learning parameters tend to converge more quickly than the slower (smaller number) parameters. Ultimately, 0.1 was selected as the learning parameter for the remainder of the analysis to balance accuracy with speed, with the algorithms converging in approximately 40 to 60 simulations with a learning parameter of 0.1.

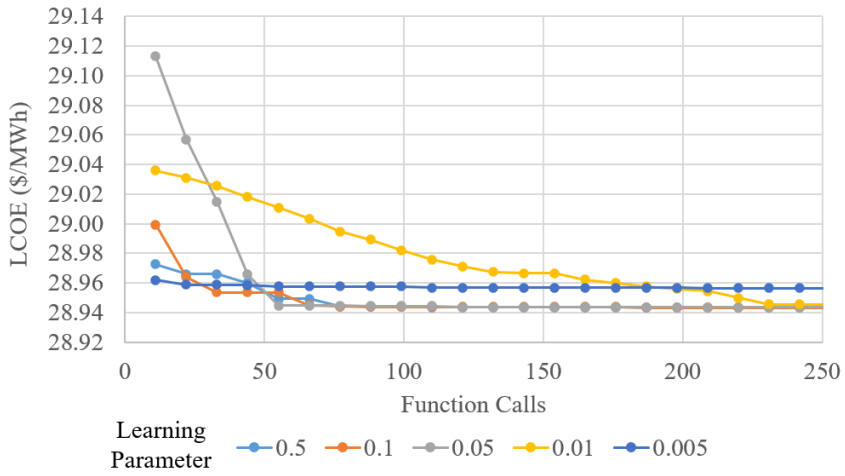

Figure 19: Particle Swarm Hyperparameter Evaluation.

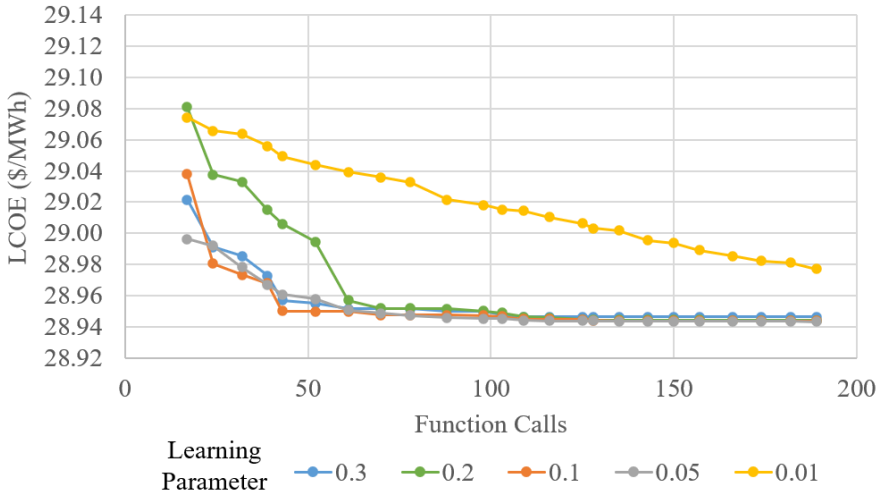

Figure 20: Genetic Algorithm Hyperparameter Evaluation.

To evaluate and compare the optimizers' relative performance with each other, the same optimization problem was solved 10 times by each optimizer with randomized starting conditions. Figure 21 and Figure 22 show the results of the repeated optimization runs for the particle swarm and genetic algorithm, respectively. In each run, the solution converges in approximately 40 to 80 model simulations.

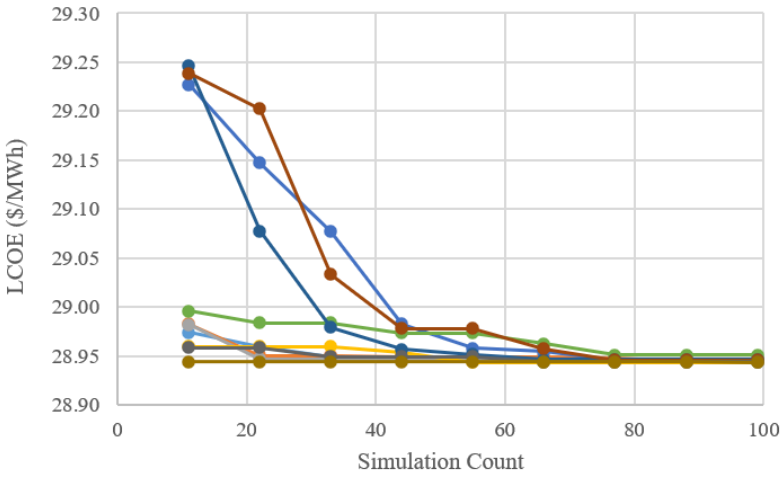

Figure 21: Particle Swarm Optimization Runs.

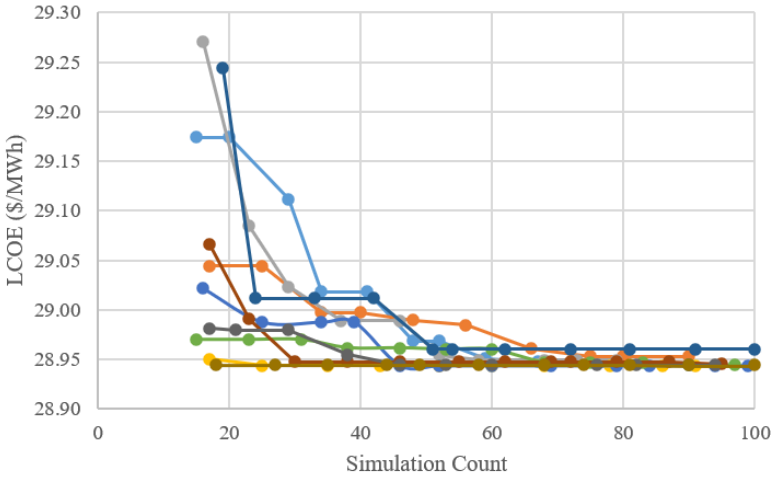

Figure 22: Genetic Algorithm Optimization Runs.

The average performance of these 10 runs was calculated for each evolutionary algorithm and compared to the average performance of the traditional gradient descent algorithm. It was found that while the evolutionary algorithms took 2 to 4 times longer to converge, they reached more optimal solutions than the traditional gradient descent algorithm. Figure 23 shows the optimizer performance comparison as a function of simulation count. The optimal LCOE reached at the end of each optimization run is plotted in Figure 24. This illustrates the greater performance of the evolutionary algorithms. It appears that the gradient descent optimizer finds local minimums and is unable to search the solution space as effectively as the evolutionary algorithms. An exhaustive analysis of traditional optimization algorithms was not performed, so there may exist others that are better suited for this application. In comparing the two evolutionary algorithms, the particle swarm algorithm gives more consistent results than the genetic algorithm. Figure 25 gives a closer view of the of the optimal LCOE reached at the end of each optimization run for these two algorithms.

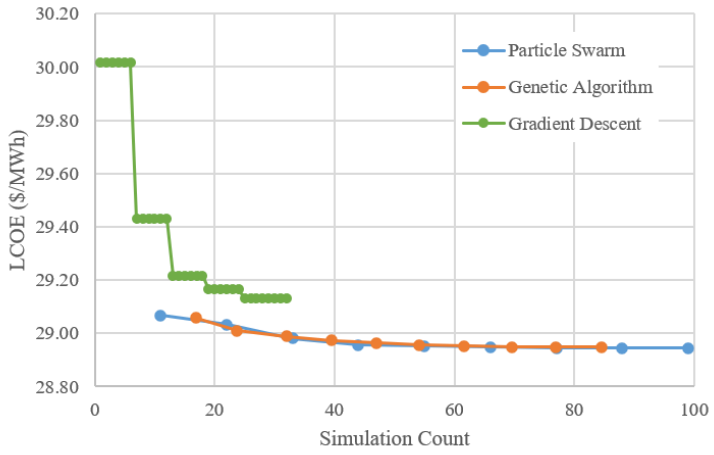

Figure 23: Optimizer Performance Comparison.

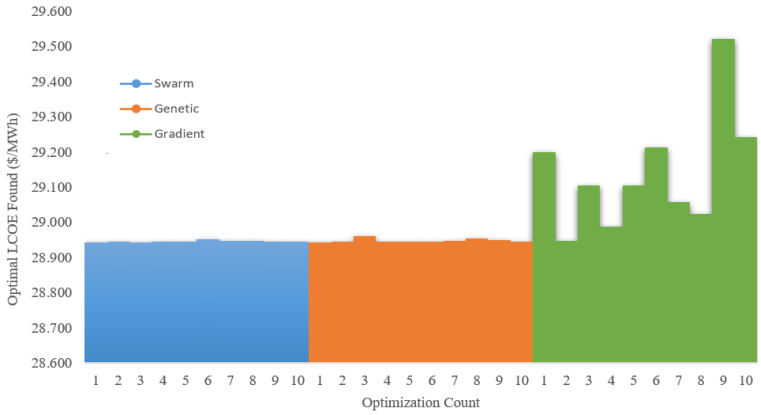

Figure 24: Optimal LCOE for Each Optimization Run.

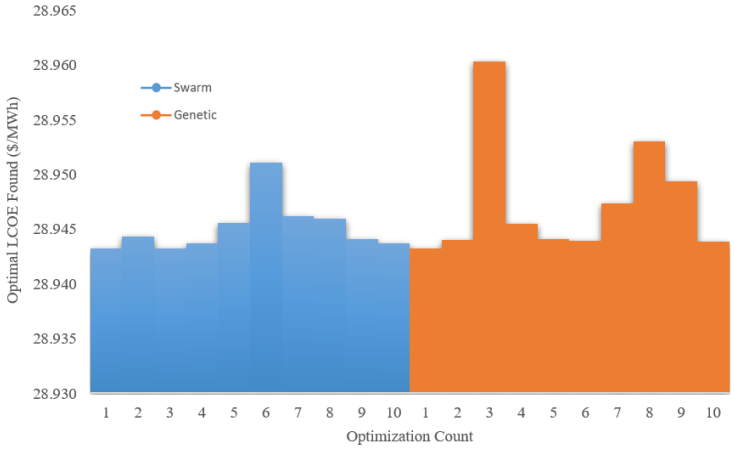

Figure 25: Optimal LCOE for Each Optimization Run Utilizing Particle Swarm and Genetic Algorithms.

Finally, in examining the parameter values reached from each optimization run, the particle swarm optimizer produced a narrower range. The optimal parameters for each optimization run are pictured in Figure 26 with the graph spanning the full parameter

ranges. In Figure 27 the graph range is narrowed to highlight the differences between the two evolutionary algorithms, with the highlighted window containing all of the particle swarm optimization runs' optimal parameters. To illustrate the optimizer effectiveness compared to a parametric sweep, this window represents 1/380 of the area of the parameter space (1/31 of the ground coverage ratio and 1/16 of the ground clearance height). To find this solution through a parametric sweep, 380 simulations would be required taking approximately 6.5 hours, whereas the particle swarm optimizer reaches the solution within 100 simulations taking approximately 1 hour and 40 minutes. Based on these tests, the particle swarm optimizer with a learning parameter of 0.1 was selected to optimize the bifacial module and tandem module cases to achieve the lowest possible LCOE configuration for each plant.

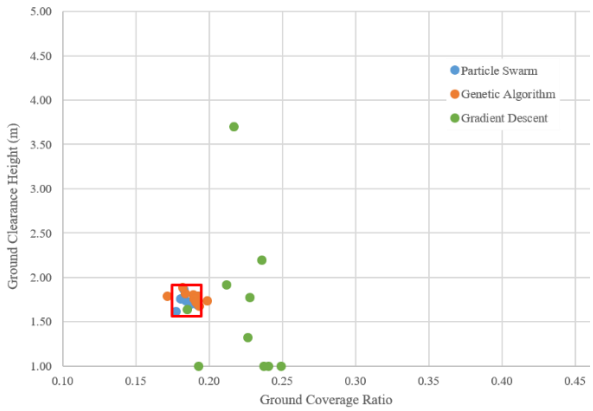

Figure 26: Optimal Parameters for Each Optimization Run.

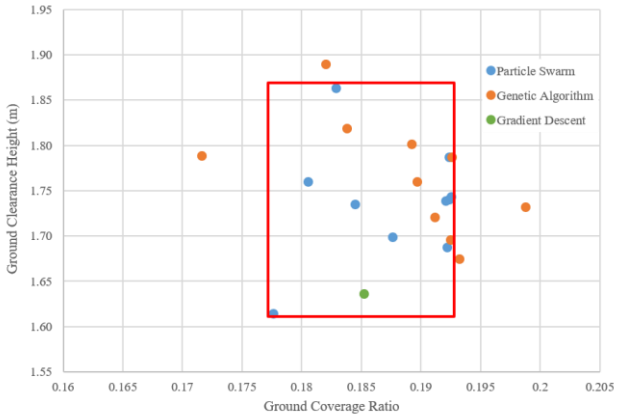

Figure 27: Optimal Parameters for Each Optimization Run (enlarged).

Bifacial Module Optimization

To determine economic viability of the future PV plant technologies studied, detailed cost breakdowns of the baseline plants were first developed, allowing for identification of key cost trade-offs and equipment-level adjustments between the baseline models and the new technology cases. For the bifacial module case, three sensitivities – GCR, module ground clearance height, and albedo grooming – were optimized using the particle swarm optimization algorithm. Because albedo can significantly affect the performance of a bifacial system by impacting the amount of light that is reflected off the ground to the

backside of the panels [22][24][25], the groomed albedo sensitivity investigated the performance and LCOE optimization of a system with a constant monthly albedo of 0.55 (the average albedo of white pebbles).

In addition to adjustments to the baseline model cost assumptions for the new bifacial modules (see Table 14), incorporation of the bifacial module sensitivities for optimization required several additional cost and model considerations. For the module ground clearance height sensitivity, items including (but not limited to) steel cost, structural design, and installation for capital costs, as well as module cleaning and other O&M costs, can be affected depending on the plant design, stringing configuration, and PV plant location. Several assumptions must be made to estimate the cost impacts of these factors and estimates for cost adders in addition to the baseline costs were informed by the literature and EPRI experts. The assumptions and cost estimates for the module ground clearance height sensitivity are listed in Table 15. Assumptions and cost estimates for the GCR and groomed albedo sensitivities are listed in Table 16 and Table 17, respectively. It should be noted that these cost factors are specifically based on the plants studied and are rough estimates. These assumed cost factors can vary and may be significant for other installations, affecting project economics.

Table 14: Bifacial Module Cost Assumptions.

Cost Factor	Assumption(s)	Cost Above Baseline
Module Cost	Current bifacial module cost based on recent EPRI studies and literature review	Adjusted module cost to \$350/W_{DC}
O&M Costs	Increase in preventative maintenance based on recent EPRI studies	\$0.3/kW-yr above baseline plant O&M

Table 15: Module Ground Clearance Height Sensitivity Cost Assumptions.

Cost Factor	Assumption(s)	Cost Above Baseline
Steel Cost	Material cost for steel is assumed to be \$0.002/W_{DC} per linear foot	Combined total: \$0.018/W_{DC} per linear meter above 1-meter ground clearance height; -\$0.006/W_{DC} per linear meter below 1-meter ground clearance height
Wind Ballasting	For every additional linear foot of vertical height, assume 2ft of steel is driven into the ground for ballasting. No additional ballasting is assumed for heights below 1 meter.	
Structural Design	Addressed by wind ballasting	
Installation	Negligible; for ground clearance heights above 7ft (2.1m), a man-lift will likely replace a skid steer at similar cost	\$0
O&M Costs	Module cleaning unaffected; for ground clearance heights above 7ft (2.1m) module maintenance is performed by a skid steer and man lift	\$0.171/kW-yr for plants with ground clearance heights above 7 ft

Table 16: GCR Sensitivity Cost Assumptions.

Cost Factor	Assumption(s)	Cost Above Baseline
Land Cost	As GCR increases or decreases, total land area will be affected. This is captured in the land prep costs.	Calculated in SAM: $5000/acre baseline cost
AC Wiring	Negligible; AC wiring length may increase with increased row-to-row distance, but not significantly.	$0
DC Wiring	Negligible; DC wiring between rows may increase, but there are fewer modules per row compared to the baseline, negating any additional DC wiring costs	$0

Table 17: Groomed Albedo Cost Assumptions.

Cost Factor	Assumption(s)	Cost Above Baseline
Land Preparation	White gravel (albedo of ~0.55) is utilized to groom PV plant land area. A cost of $2.75/ft^3 is assumed for white gravel at each plant with a gravel coverage depth of 0.5".	$5,000/acre

These cost assumptions were incorporated into the SAM model for each plant location, using the original GCR and ground clearance height for the Southwest, Southeast, and Midwest PV plants. The resulting "non-optimized" performance and LCOE results were calculated and then compared to the optimized results utilizing the particle swarm algorithm in PySAM to determine the optimal GCR and ground clearance height resulting in the lowest LCOE at each plant array. Optimized GCR and bifacial module ground clearance height values compared to the baseline are listed in Table 18.

Table 18: Baseline and Optimized GCR and Module Ground Clearance Height for Bifacial Modules.

PV Plant		GCR		Module Ground Clearance Height (m)	
		Baseline	Optimized	Baseline	Optimized
Southwest Plant	Array 1	0.463	0.192	1.00	1.82
	Array 2	0.463	0.189	1.00	1.74
	Array 3	0.493	0.185	1.00	1.57
Southeast Plant	Array 1	0.543	0.296	1.00	1.00
	Array 2	0.543	0.313	1.00	1.00
	Array 3	0.543	0.345	1.00	1.00
	Array 4	0.211	0.192	1.00	1.30
Midwest Plant		0.487	0.243	1.00	1.00

For each case, GCR decreases significantly when optimized to reduce row-to-row shading loss. This signifies that, with the estimated land and preparation costs listed in Table 16, it is economically advantageous to increase row-to-row spacing for these three plants under these conditions. However, if land cost assumptions were to increase, optimized GCR may change as a result. For bifacial module ground clearance height, the results show the saturation effect of backside performance gains identified in the literature review. For SAT arrays in the Southwest and Southeast plants, average optimal ground clearance height is approximately 1.7 meters and 1.3 meters, respectively. For all fixed-tilt arrays studied, average optimal ground clearance height is 1 meter. These values are attributed to the differences in tracking technology, combined with locational irradiance and albedo effects, where average annual albedo for the Southwest, Southeast and Midwest plants is about 0.21, 0.14, and 0.26, respectively. As a result, an average bifacial module ground clearance height of 1.7 meters for the Southwest plant is economically viable due to the increased backside energy gain available resulting from tracking and higher annual albedo and irradiance. Contrastingly, the lower albedo and irradiance of the Southeast location does not make it economically viable to optimize fixed-tilt ground clearance height beyond 1 meter. Instead, only the Southeast plant's SAT array's ground clearance height is increased. As an entirely fixed-tilt installation, the Midwest plant optimized ground clearance height remains at 1 meter despite elevated albedo, due to the lower irradiance profile of the Midwest location. These energy differences between bifacial SAT systems and bifacial fixed-tilt systems align with previous conclusions by NREL.

Optimized LCOE results are listed and compared to baseline and non-optimized LCOEs in Table 19. With the optimized GCR and ground clearance height, average LCOE results decreased by 3.9% to 6.6% when compared to the baseline values. For Array 3 of the Southwest plant, LCOE results for the optimized SAT bifacial array decreased by nearly 10% compared to the baseline, monofacial SAT array.

Table 19: Baseline, Non-Optimized, and Optimized LCOE Results for Bifacial Modules.

PV Plant		Nominal LCOE ($/MWh)		
		Baseline	Non-Optimized	Optimized
Southwest Plant	Array 1	35.62	37.11	35.18
	Array 2	35.62	37.11	34.91
	Array 3	38.95	37.71	35.19
Southeast Plant	Array 1	53.05	51.14	50.17
	Array 2	52.15	50.32	49.79
	Array 3	51.90	50.76	50.19
	Array 4	47.50	45.14	45.10
Midwest Plant		58.02	55.68	54.03

Highlighting the value of optimizing plant design when possible, the LCOE for these models with optimized designs was compared with those of the non-optimized bifacial cases that used the same GCR and ground clearance height as the baseline plant. LCOE for the optimized plants was between 0.9% and 6.1% lower compared to the non-optimized plants. The range of LCOE improvement between plants can be attributed to

original plant design and size. For plants where original plant design was not optimal for bifacial modules, greater opportunities exist to improve energy optimization and, as a result, LCOE.

Table 20 shows the optimized annual energy production for the three plants. In all cases, the optimized configurations resulted in increased annual energy output over both the baseline and non-optimized cases, indicating that the cost increases associated with increased ground clearance height and GCR were offset by the increased energy output. These results show how system energy can be improved via GCR and ground clearance height when optimized alongside system costs to achieve the lowest possible LCOE.

Table 20: Baseline, Non-Optimized, and Optimized Annual Energy Production for Bifacial Modules.

PV Plant		Annual Energy Production (MWh)		
		Baseline	Non-Optimized	Optimized
Southwest Plant	Array 1	89,914	90,674	99,087
	Array 2	25,688	25,932	28,313
	Array 3	30,094	31,370	34,420
Southeast Plant	Array 1	367	383	394
	Array 2	373	389	396
	Array 3	409	425	432
	Array 4	449	471	474
Midwest Plant		4,313	4,517	4,701

To understand the implications of different bifacial module specifications on optimization results, the same set of optimization analyses were run on the second bifacial module developed based on the informational interview datasheet collected. Table 21 through Table 23 show these results. Despite differences in module specifications such as power rating and module area, the optimization results for the two bifacial modules were quite similar.

Table 21: Baseline and Optimized GCR and Module Ground Clearance Height for Bifacial Module 2.

PV Plant		GCR		Module Ground Clearance Height (m)	
		Baseline	Optimized	Baseline	Optimized
Southwest Plant	Array 1	0.463	0.191	1.00	1.69
	Array 2	0.463	0.184	1.00	1.73
	Array 3	0.493	0.186	1.00	1.63
Southeast Plant	Array 1	0.543	0.297	1.00	1.00
	Array 2	0.543	0.311	1.00	1.00
	Array 3	0.543	0.345	1.00	1.00
	Array 4	0.211	0.190	1.00	1.25
Midwest Plant		0.487	0.226	1.00	1.00

Table 22: Baseline, Non-Optimized, and Optimized LCOE Results for Bifacial Module 2.

PV Plant		Nominal LCOE ($/MWh)		
		Baseline	Non-Optimized	Optimized
Southwest Plant	Array 1	35.62	37.55	35.31
	Array 2	35.62	37.55	35.31
	Array 3	38.95	38.13	35.54
Southeast Plant	Array 1	53.05	51.90	50.89
	Array 2	52.15	51.11	50.52
	Array 3	51.90	51.20	50.63
	Array 4	47.50	46.20	46.14
Midwest Plant		58.02	55.97	54.29

Table 23: Baseline, Non-Optimized, and Optimized Annual Energy Production for Bifacial Module 2.

PV Plant		Annual Energy Production (MWh)		
		Baseline	Non-Optimized	Optimized
Southwest Plant	Array 1	89,914	89,610	97,828
	Array 2	25,688	25,603	27,997
	Array 3	30,094	31,040	34,139
Southeast Plant	Array 1	367	377	387
	Array 2	373	382	390
	Array 3	409	422	429
	Array 4	449	462	466
Midwest Plant		4,313	4,489	4,680

An albedo grooming scenario was also incorporated into the models and optimized using the optimization algorithm to understand the potential impact of increasing plant albedo to maximize bifacial module gain. Optimized GCR and ground clearance heights, as well as LCOE and annual energy production results from the albedo grooming optimization, are compared to the ungroomed albedo case in Table 24 and Table 25. Compared to the ungroomed albedo case, optimal GCR values for the albedo grooming sensitivity increased slightly, resulting in a smaller plant area, while optimal bifacial module ground clearance height decreased. This signifies a point at which decreasing GCR to mitigate row-to-row shading no longer becomes cost effective due to the increased land preparation costs associated with albedo grooming.

Table 24: Optimized GCR and Module Ground Clearance Heights for the Ungroomed and Groomed Albedo Cases.

PV Plant		Optimized GCR		Optimized Ground Clearance Height (m)	
		Ungroomed	Groomed	Ungroomed	Groomed
Southwest Plant	Array 1	0.192	0.221	1.82	1.77
	Array 2	0.189	0.214	1.74	1.70

	Array 3	0.185	0.225	1.57	1.55
Southeast Plant	Array 1	0.296	0.374	1.00	1.00
	Array 2	0.313	0.382	1.00	1.00
	Array 3	0.345	0.382	1.00	1.00
	Array 4	0.192	0.238	1.30	1.12
Midwest Plant		0.243	0.308	1.00	1.00

Table 25: Optimized LCOE and Annual Energy Production for the Ungroomed and Groomed Albedo Cases.

PV Plant		**Nominal LCOE ($/MWh)**		**Annual Energy Production (MWh)**	
		Ungroomed	**Groomed**	**Ungroomed**	**Groomed**
Southwest Plant	Array 1	35.18	35.99	99,087	104,266
	Array 2	34.91	35.72	28,313	29,800
	Array 3	35.19	35.99	34,420	35,741
Southeast Plant	Array 1	50.17	50.97	394	420
	Array 2	49.79	50.48	396	423
	Array 3	50.19	50.89	432	456
	Array 4	45.10	46.12	474	495
Midwest Plant		54.03	54.99	4,701	4,949

With an increased albedo, annual energy production of the albedo-groomed sensitivity cases increased by an average of 4.8% to 5.9% compared to the ungroomed albedo cases' optimized energy. However, this increased energy yield is not enough to overcome the additional land preparation cost assumption associated with groomed albedo, resulting in slightly higher LCOE results for the albedo-groomed sensitivity compared to the optimized, ungroomed albedo LCOE results. These results show the trade-off between different approaches and associated costs to increase plant output. However, they are dependent on the assumptions made for this analysis and further sensitivities could reveal different tipping points depending on cost assumptions.

Tandem Module Optimization

Due to the uncertainty around future tandem module costs, three tandem module cost sensitivities (shown in Table 26) ranging from optimistic to conservative were developed based on a range of cost adder assumptions reported by Sofia et al. (2019) [10] applied to the baseline c-Si module cost assumption. The GCR cost adders developed for bifacial modules and listed in Table 16 were incorporated into each tandem module model case for optimization. Other optimization factors, such as module ground clearance height and albedo grooming, were not considered for tandem modules because their impact on performance was expected to be negligible.

Table 26: Tandem Module Cost Assumptions.

Cost Factor	Assumption(s)	Cost Above Baseline
Module Cost	Based on costs reported by Sofia et al. (2019) [10]	Adjusted module cost to \$360/kW$_{DC}$, \$400/kW$_{DC}$ and \$440/kW$_{DC}$

Optimized GCR for the three tandem module cost sensitivities are listed in Table 27. Compared to baseline GCR values, optimal GCR decreased for all three plants, decreasing more as the assumed module price increased. These results also show the trade-off between tandem module price and GCR: as tandem module price increases for each scenario, GCR decreases to increase energy production, even with the cost of additional land. As a result, annual energy production of the optimized plant configuration for each case increases as tandem module costs increase (see Table 28), though LCOE also increases as the tandem module cost increases (see Table 29).

Table 27: Baseline and Optimized GCR for Tandem Modules at Three Representative Module Costs.

PV Plant		Baseline GCR	Optimized GCR		
			\$360 Tandem Module	\$400 Tandem Module	\$440 Tandem Module
Southwest Plant	Array 1	0.463	0.198	0.198	0.196
	Array 2	0.463	0.199	0.198	0.197
	Array 3	0.493	0.193	0.191	0.187
Southeast Plant	Array 1	0.543	0.332	0.324	0.325
	Array 2	0.543	0.362	0.357	0.351
	Array 3	0.543	0.362	0.361	0.355
	Array 4	0.211	0.191	0.189	0.186
Midwest Plant		0.487	0.289	0.285	0.281

Table 28: Comparison of the Baseline, Non-Optimized, and Optimized Tandem Module Annual Energy Production for Three Representative Costs.

PV Plant		Annual Energy Production (MWh)				
		Baseline	Non-Optimized Tandem Module	Optimized		
				\$360 Tandem Module	\$400 Tandem Module	\$440 Tandem Module
Southwest Plant	Array 1	89,914	92,333	97,236	97,240	97,255
	Array 2	25,688	26,381	27,780	27,781	27,785
	Array 3	30,094	31,637	33,975	33,981	33,993
Southeast Plant	Array 1	367	390	394.9	395.0	395.0
	Array 2	373	395	398.0	398.0	398.1
	Array 3	409	423	427.8	427.8	427.9
	Array 4	449	475	476.3	476.4	476.5

Midwest Plant	4,313	4,487	4,554	4,555	4,555

Table 29: Comparison of the Baseline and Optimized Tandem Module LCOE for Three Representative Costs.

PV Plant		Nominal LCOE ($/MWh)			
		Baseline	Optimized		
			$360 Tandem Module	$400 Tandem Module	$440 Tandem Module
Southwest Plant	Array 1	35.62	34.33	35.73	37.13
	Array 2	35.62	34.33	35.73	37.13
	Array 3	38.95	34.50	35.90	37.30
Southeast Plant	Array 1	53.05	49.79	51.98	54.17
	Array 2	52.15	49.34	51.52	53.69
	Array 3	51.90	49.58	51.81	54.04
	Array 4	47.50	44.09	45.91	47.73
Midwest Plant		58.02	55.10	57.45	59.80

Optimizing tandem module GCR led to a decrease in LCOE for the $360/kW$_{DC}$ tandem module case by an average of 5.0% to 6.2% compared to the baseline LCOE. Additionally, most optimized plants' LCOE decreased for the $400/kW$_{DC}$ tandem module cost, compared to the baseline, but increased once tandem module cost was raised to $440/kW$_{DC}$. These results show that there may exist a tandem module cost tipping point where a utility-scale tandem module plant may achieve a lower LCOE than monofacial c-Si or CdTe plants. However, this tipping point will vary by plant location and other economic factors.

Increased Voltage Architectures

To analyze plant economics of increased voltage architectures, several cost adders were considered and incorporated into the economic model. Increased inverter cost is expected to be a significant portion of the additional cost required for increased plant voltage architectures. For this analysis, inverter cost was assumed to increase with each voltage step from 2000V, 2500V, and 3000V. This increase in cost is due to the need for additional research and development, wiring type changes, development of robust internal hardware, and potential need for metal clad inverter enclosures to accommodate increased voltage architectures. However, this cost is assumed to be greatest when making the initial step from 1500V to 2000V, as PV inverters at this voltage do not yet exist. For 2500V and 3000V inverters, costs are assumed to increase at a slower rate as the effort and components to manufacturer a 2000V inverter may be utilized for 2500V and 3000V steps. While this analysis assumed R&D efforts would carry over from 2000V to 2500V and 3000V inverter costs due to the use of the same internal components, there exists a voltage limit where inverter components would need to be upgraded to accommodate higher voltages, requiring additional R&D efforts by inverter manufacturers that would likely impact inverter costs. Assumed inverter costs for the three plants are shown in Table 30.

Table 30: Increased Voltage Inverter Cost Assumptions.

PV Plant	Inverter Cost ($/kW$_{AC}$)			
	Baseline Inverter	2000V	2500V	3000V
Southwest Plant	88.0	110.5	120.5	128.5
Southeast/Midwest Plants	103.0	125.5	135.5	143.0

Another key impact of higher-voltage architectures on plant economics would be the reduction in the number of combiner boxes needed – because a single string can accommodate higher voltages and, therefore, more modules, there are fewer strings within the plant, resulting in a need for fewer combiner boxes. Because SAM does not specifically account for the number and associated costs of combiner boxes within the model, the number of combiner boxes for each voltage step was calculated outside of the model to understand the impact of fewer combiner boxes required due to increased voltage. This was done by comparing the number of strings at 2000V, 2500V, and 3000V to the baseline number of strings. From there, the reduction in the number of combiner boxes required for each voltage step was calculated, assuming 24 strings per combiner box for CdTe and 8 strings per combiner box for c-Si, based on the differences in the short circuit currents and power ratings of the two module types, as well as assumptions about the combiner box fuse ratings and the utilization of combiner boxes for utility-scale plants. The number of strings per combiner box can vary depending on the current rating of fuses, number of inputs, and utilization of each box. Savings were then quantified using a combiner box cost based on EPRI's 2020 solar cost and performance report [20] and verified through informational interviews and incorporated into each plant's economic model for all three plant voltages. Savings assumptions are shown in Table 31. These cost savings reflect component savings from fewer combiner boxes only, and do not account for other potential cost considerations that may arise, such as less installation labor and material costs for PV source circuits and PV output circuits.

Table 31: Increased Voltage Architecture Combiner Box Savings Assumptions.

PV Plant		Number of Combiner Boxes				Cost Savings ($/kW$_{DC}$)			
		Baseline	2000V	2500V	3000V	Baseline	2000V	2500V	3000V
Southwest Plant	Array 1	617	478	365	279	-	-4.6	-8.7	-11.8
	Array 2	177	144	92	80	-	-3.6	-11.8	-11.8
	Array 3	162	103	98	92	-	-6.6	-6.0	-5.8
Southeast Plant	Array 1	6	3	3	2	-	-15.4	-12.9	-15.1
	Array 2	6	3	3	2	-	-15.4	-12.9	-15.1
	Array 3	7	3	3	3	-	-18.5	-15.4	-13.4
	Array 4	6	3	3	2	-	-15.4	-12.9	-15.1
Midwest Plant		40	28	23	19	-	-5.0	-6.8	-8.7

Additional O&M costs were also included for the 2000V, 2500V, and 3000V cases. To account for the difference in O&M equipment, training, and specialization as voltage increases, overall baseline O&M costs were increased by 2.5%.

LCOE results for the associated cost assumptions for each voltage step are shown in Table 32. Compared to the baseline case, these results show an average increase in

LCOE of 0.5%, 1.1%, and 1.5% for the 2000V, 2500V, and 3000V cases, respectively, though in the case of the Southeast plant there is a slight decrease in LCOE for the 2000V case. In general, the increase in LCOE is due to the increased inverter costs assumed for each voltage step outweighing the savings in combiner boxes and slight increase in plant output due to the reduced losses in DC and AC wiring.

Table 32: LCOE for Increased Voltage System Architectures Compared to the Baseline Utilizing Scaled Inverter Costs.

PV Plant		Nominal LCOE ($/MWh)			
		Baseline	2000V	2500V	3000V
Southwest Plant	Array 1	35.62	36.17	36.25	36.33
	Array 2	35.62	36.20	36.13	36.32
	Array 3	38.95	39.46	39.74	39.95
Southeast Plant	Array 1	53.05	52.73	53.28	53.34
	Array 2	52.15	51.81	52.27	52.42
	Array 3	51.90	51.28	51.76	52.14
	Array 4	47.50	47.06	47.43	47.47
Midwest Plant		58.02	58.56	58.85	59.08

To bookend the analysis and further understand the potential benefits of increased voltage architectures, a second case was analyzed assuming that inverter manufacturers were eventually able to develop higher-voltage inverters at the same or similar cost as today. Each economic model was evaluated utilizing the baseline inverter cost, while still accounting for changes to system losses, O&M costs, and the number of combiner boxes. The results of this analysis are listed in Table 33. With inverter costs held constant, increasing plant voltages to 2000V, 2500V, and 3000V results in a decrease in LCOE by an average of 1.5%, 1.8% and 2.1%, respectively, compared to the baseline. These results show the potential economic advantages of increasing utility-scale plant voltage architectures if inverter cost increases can be minimized as manufacturers develop future higher-voltage inverters.

Table 33: LCOE for Increased Voltage System Architectures Compared to the Baseline Utilizing Constant Inverter Costs.

PV Plant		Nominal LCOE ($/MWh)			
		Baseline	2000V	2500V	3000V
Southwest Plant	Array 1	35.62	35.42	35.17	34.99
	Array 2	35.62	35.45	35.06	34.98
	Array 3	38.95	38.66	38.59	38.52
Southeast Plant	Array 1	53.05	51.72	51.82	51.55
	Array 2	52.15	50.82	50.85	50.66
	Array 3	51.90	50.38	50.46	50.55
	Array 4	47.50	46.24	46.24	46.01
Midwest Plant		58.02	57.34	57.10	56.91

Module-Level Power Electronics

One of the major cost considerations of incorporating MLPE is the component cost of microinverters or DC-DC optimizers. Cost quotes for both microinverters and DC-DC optimizers were gathered, yielding $198 per unit and $125 per unit, respectively. Because this cost is representative of commercial and residential-scale systems only, a 50% discount was assumed given the number of microinverters or DC-DC optimizers that would be ordered to deploy these technologies on a utility-scale system. With the discount applied, microinverter and DC-DC optimizer costs were assumed to be $99 per unit and $62.50 per unit, respectively. For the microinverter cases, these costs were incorporated on a $/$W_{AC}$ basis, replacing the costs of the baseline inverters. For the DC-DC optimizer cases, costs were incorporated on a $/$W_{AC}$ basis, added to the overall inverter cost since DC-DC optimizers do not replace the need for inverters. In addition to component costs, additional labor for installation, as well as increased O&M costs were accounted for with both microinverters and DC-DC optimizers. These cost adders are representative of the need to individually install and maintain/assess each component in the field compared to the baseline case. They are listed in Table 34.

Table 34: MLPE Cost Assumptions.

Cost Factor	Assumption(s)	Cost Above Baseline
Mircroinverter Equipment	50% discount on typical commercial/residential components	$99/unit or $0.28/$W_{AC}$ replaces inverter cost
Microinverter Installation	Accounts for additional installation time/labor	$0.0125/$W_{DC}$ added
DC-DC Optimizer Equipment	50% discount on typical commercial/residential components	$62.5/unit or $0.16-0.24/$W_{AC}$ added to inverter cost
DC-DC Optimizer Installation	Accounts for additional installation time/labor	$0.0075/$W_{DC}$ added
O&M Costs	Additional maintenance labor needed to service each microinverter or optimizer	$1.0/kW-yr added

The cost adders for microinverters and DC-DC optimizers were incorporated into SAM and the LCOE for each configuration was calculated, as shown in Table 35.

Table 35: LCOE Results for the Microinverter Case and DC-DC Optimizer Case Compared to the Baseline.

PV Plant		Nominal LCOE ($/MWh)		
		Baseline	Microinverter	DC Optimizer
Southwest Plant	Array 1	35.62	42.00	41.84
	Array 2	35.62	42.00	41.84
	Array 3	38.95	47.56	46.28
Southeast Plant	Array 1	53.05	66.91	64.05
	Array 2	52.15	64.71	62.96
	Array 3	51.90	64.87	62.83
	Array 4	47.50	57.77	56.49

Midwest Plant	58.02	71.48	69.63

As expected, the LCOE for microinverters and DC-DC optimizers is significantly higher than the baseline, increasing by an average of 22.2% and 19.4%, respectively, due to the increase in component costs combined with minimal impact on annual energy production (see Table 36). Since shading events are excluded from these utility-scale models as typical utility-scale PV plants are designed to mitigate objects that may cause partial shading events, some of the key benefits of microinverters are not captured in the model. Additionally, the SAM model does not capture dynamic module mismatch and PV plant reliability as part of this analysis. If these characteristics were captured in future analyses, the economics for microinverters and DC-DC optimizers may improve compared to a baseline that considered the negative impacts of these characteristics. However, for microinverters and DC-DC optimizers to become economically advantageous, further reduction in component costs are likely also needed.

Table 36: Annual Energy Production of Microinverter and DC-DC Optimizer Cases Compared to the Baseline.

PV Plant		Annual Energy Production (MWh)		
		Baseline	Microinverter	DC Optimizer
Southwest Plant	Array 1	89,914	88,538	89,732
	Array 2	25,688	25,295	25,636
	Array 3	30,094	29,797	30,087
Southeast Plant	Array 1	367	369	366
	Array 2	373	375	373
	Array 3	409	418	408
	Array 4	449	450	448
Midwest Plant		4,313	4,270	4,305

Milestone Accomplishments

Milestone 3.1: Incorporation of new technologies into model was achieved with the development of new technology components in the SAM models and incorporation of technology cost assumptions for these technologies and other impacted components.

Milestone 3.2: Ability of model to run multiple runs and iteratively approach efficient frontier was achieved through the selection and development of the particle swarm optimizer in PySAM.

Milestone 3.4: Model capable of multi-variate optimization was achieved as the particle swarm optimizer was used to identify an optimized plant configuration for GCR and ground clearance height while considering different plant albedo scenarios.

Task 4: Improved Modeling of New Technologies

Throughout the project, opportunities were identified to improve the representation of the new technologies within the model. Updated bifacial module datasheets were acquired and incorporated into custom modules within SAM to better capture the characteristics of current cutting edge module technologies and seasonal albedo factors were incorporated

into the model's weather files to capture the impact of varying albedo over the course of a year. Both of these were incorporated into the bifacial modeling analysis and optimization. In addition, detailed analysis was also conducted to better understand the impact of temperature coefficients and linear versus non-linear shading on bifacial module model results.

Temperature Coefficient Analysis

A temperature coefficient analysis was conducted to better understand the impact of the temperature coefficients of different module types on overall plant performance. Both of the custom bifacial modules developed in SAM for this project were analyzed to understand the difference across the two technologies as well.

For this comparison, each bifacial module base case was modeled to establish baseline bifacial performance, maintaining the original plant GCR and 1-meter ground clearance height. The bifacial c-Si module's temperature coefficients were then changed to reflect the temperature coefficients of a CdTe module, which are typically found to be less impacted by temperature changes that c-Si modules (see Table 37).

Table 37: Original OEM Bifacial Module and CdTe Temperature Coefficients.

Temperature Coefficient	Bifacial Module #1	Bifacial Module #2	CdTe Module
Temperature Coefficient of V_{oc} (%/^{o}C)	-0.26	-0.284	-0.28
Temperature Coefficient of I_{sc} (%/^{o}C)	0.05	0.05	0.04
Temperature Coefficient of P_{mp} (%/^{o}C)	-0.34	-0.35	-0.32

These revised models were then simulated for the Southwest plant and compared to understand how much of the performance gains or losses observed when substituting bifacial modules for CdTe modules were due to inherent temperature-related impacts when switching from CdTe to bifacial c-Si modules.

It was found that the change in temperature coefficients impacted annual plant output by 0.6%-1% and monthly plant output by 0.2%-1.4%. As a check, a sensitivity using one of the two bifacial modules was also conducted for the Southeast plant, which generally experienced less extreme temperatures and, therefore, was assumed would be less impacted by changes in temperature coefficients. Results are displayed in Table 38 in terms of performance gain/loss using the CdTe temperature coefficients in place of the bifacial module base case with OEM temperature coefficients.

Table 38: Increase in Monthly Bifacial Energy Output Utilizing CdTe Temperature Coefficients in Place of OEM Temperature Coefficients.

Month	Southwest Plant		Southeast Plant
	Bifacial Module #1 with Adjusted Temperature Coefficients	Bifacial Module #2 with Adjusted Temperature Coefficients	Bifacial Module #1 with Adjusted Temperature Coefficients
January	0.35%	0.58%	0.21%

February	0.30%	0.52%	0.22%
March	0.40%	0.68%	0.28%
April	0.44%	0.76%	0.34%
May	0.52%	0.91%	0.47%
June	0.77%	1.28%	0.70%
July	0.78%	1.29%	0.74%
August	0.86%	1.42%	0.75%
September	0.77%	1.27%	0.66%
October	0.57%	0.95%	0.41%
November	0.47%	0.78%	0.37%
December	0.26%	0.45%	0.30%
Total	0.58%	0.97%	0.21%

The associated performance impact of CdTe temperature coefficients versus c-Si temperature coefficients is largely dependent on the original module-specific temperature coefficients. Bifacial Module #1 shows lower performance gains when its temperature coefficients are adjusted to match CdTe coefficients given that changes between the different coefficients balance each other, with the temperature coefficient of V_{oc} lower for the bifacial module but the temperature coefficient of P_{mp} higher. Bifacial Module #2 shows greater performance gains as the change between its OEM temperature coefficients and the CdTe coefficients are greater. As expected, the performance gains with the more advantageous CdTe temperature coefficients are greater in the Southwest plant than the Southeast plant due to the less extreme temperatures experienced at the Southeast plant. In all three cases analyzed, the performance gains are highest in the hotter summer months.

Note that this analysis was conducted to better understand the results of decreased plant output observed in the initial incorporation of bifacial modules in the Southwest plant but does not represent a viable technology change for bifacial modules at this time.

Linear versus Non-Linear Shading Analysis

A linear versus non-linear shading analysis was also conducted to understand the performance differences between CdTe linear shading response and c-Si-associated non-linear shading response. For this comparison, the Bifacial Module #2 case was used to establish baseline bifacial performance, maintaining the original plant GCR and 1-meter ground clearance height. Self-shading within SAM was then changed from non-linear (the typical assumption for c-Si modules) to linear shading (the typical assumption for CdTe modules), with no other changes to module characteristics. This self-shading change allows for the bifacial c-Si cells shading response to be calculated in the same manner as CdTe cell shading response.

These scenarios were simulated for the Southwest and Southeast plants to understand differences between fixed-axis and SAT arrays, with results displayed in Table 39. Percentages are given in performance gain over the baseline Bifacial Module #2 case. These results point to the losses associated with shading, particularly for the Southwest plant, where backtracking is not present on the original SAT CdTe portions of the plant. These shading response results contributed to the motivation for adding backtracking to the Southwest plant, helping to mitigate row-to-row shading. In contrast, though

performance gains are observed utilizing linear shading response for the Southeast plant, this plant employs mainly fixed-tilt arrays and already utilizes backtracking where applicable. Therefore, any performance gains observed are intrinsic to the differences between c-Si and CdTe cell shading responses, which are not able to be changed unless manufacturing processes and module/cell design of c-Si is revolutionized.

Note that this analysis was conducted to better understand the results of decreased plant output observed in the initial incorporation of bifacial modules in the Southwest plant but does not represent a viable technology change for bifacial modules at this time.

Table 39: Increase in Monthly Bifacial Energy with Linear Shading Response Instead of Non-Linear Shading Response.

Month	Southwest Plant	Southeast Plant
	Bifacial Module #2 with Linear Shading Response	Bifacial Module #2 with Linear Shading Response
January	17.35%	2.19%
February	11.09%	1.17%
March	9.03%	0.86%
April	8.04%	0.79%
May	10.34%	0.90%
June	7.28%	0.97%
July	5.65%	1.01%
August	8.65%	1.01%
September	10.21%	1.02%
October	14.47%	1.22%
November	9.57%	2.04%
December	11.98%	2.06%
Total	9.73%	1.19%

Milestone Accomplishments

Milestone 2.3: Modeling approach defined and Milestone 4.1: Demonstrated capability of improved modeling fidelity of bifacial modules was achieved through analysis of bifacial module response to different modeling assumptions and the incorporation of updated bifacial module technologies and seasonal albedo adjustments into the plant models and results.

Milestone 4.2 (stretch): Demonstrated capability of improved modeling fidelity of tandem modules was not achieved over the course of this project. While initial conversations took place around modeling options for better representing tandem modules, timeline and budget constraints limited the ability to achieve this stretch goal.

Significant Accomplishments and Conclusions:

This project developed a thorough analysis of potential LCOE impacts of several novel PV technologies and developed a tool to investigate the tradeoffs and optimal design among key plant design characteristics. Three of the four technologies evaluated – bifacial modules, tandem modules, and increased plant voltages – resulted in increased

plant output compared to the baseline plants and, in optimized cases, potential reductions in LCOE.

LCOE reductions up to 5-7% compared to the baseline were seen when the GCR and module ground clearance height were optimized for bifacial modules and tandem modules, demonstrating tradeoffs between maximizing plant output with equipment and plant costs. While this did not achieve the stated project goal of >20% reduction in LCOE from baseline costs, it does demonstrate a continued trend in decreasing plant costs and improving performance. These results also assumed that all other plant costs remained the same as those seen today. In actuality, costs associated with balance of plant equipment, labor, and O&M also continue to fall, so achieving a reduction of greater than 20% from today's baseline LCOE values is a greater possibility when considering these continued cost decreases in addition to novel plant technologies and designs.

This project also demonstrated the importance of a coordinated strategy between novel PV technologies and plant design considerations such as GCR, module ground clearance height, and albedo when trying to achieve LCOE reductions for PV plants.

Some key takeaways for the novel PV technologies analyzed are summarized below.

Bifacial Module Key Takeaways

- Adding bifacial modules without plant design optimization did not guarantee greater plant performance. This was especially true in the case where bifacial modules were replacing CdTe modules without backtracking technology due to differences in cell shading responses.
- In all cases, optimized GCR was reduced (row spacing increased) compared to the baseline plant design when land was not constrained in order to maximize plant output.
- Increasing the ground clearance height of SAT systems to 1.3 to 1.7 meters proved to be cost effective, based on the assumed steel costs and locational albedo.
- Grooming plant albedo resulted in increased LCOE compared to a plant without grooming due to the assumed cost of white gravel and additional land preparation, but it also achieved increased plant output.

Tandem Module Key Takeaways

- A simple methodology for the creation of a utility-scale monofacial 4T tandem module in SAM was developed, allowing for estimations of tandem module performance impacts.
- Optimal GCR for tandem modules decreased by an average of 43% compared to the baseline as additional plant output from reduced shading offset the cost of additional land.
- Decreasing GCR resulted in increased energy production by tandem modules but was not enough to overcome increased tandem module costs beyond the \$400/W_{DC} tandem module cost sensitivity.
- At a cost sensitivity of \$360/W_{DC}, tandem module systems in this analysis resulted in LCOEs below the baseline, signifying the potential for tandem module systems if large-scale tandem modules can be manufactured at low cost.

Increased Plant Voltages Key Takeaways

- Estimated specifications for custom 2000V, 2500V, and 3000V inverters were developed based upon data collected from 90+ inverter datasheets and conversations with industry experts.
- Inverter cost for 1500V+ systems is critical in determining the economic viability of increased system voltage architectures. With the increased inverter costs assumed, LCOE increased by about 1% on average, but when inverter costs were assumed to be able to achieve current $/kW$_{AC}$ prices for 1500V inverters, LCOE decreased by an average of about 2%.
- Plant capacity factor improved slightly due to reduced losses in DC and AC wiring.
- The specifications and costs of future 2000V, 2500V, and 3000V inverters are unknown, and may change as technology improvements are made.
- Codes and standards may become a key hurdle limiting adoption of increased plant voltage architectures.

Module-Level Power Electronics Key Takeaways

- Although module-level power electronics can be beneficial for residential and commercial systems where shading events and permanent shading may occur, typical utility-scale plants are designed to avoid permanent shading events.
- SAM does not account for real-world reliability factors that might make the LCOE of microinverters and/or DC optimizers more competitive when compared to a string inverter or central inverter system.
- The combination of these factors results in little improvement in annual energy production, while increasing system costs.
- A follow-on study would be needed to understand the performance and LCOE viability of MLPE components at the utility scale. This follow-on study would evaluate a dynamically evolving module mismatch loss percentage rather than the current constant loss percentage assumption to understand if there are benefits associated with these components as a PV plant ages and ultimately degrades, leading to greater possibility for module mismatch.

Milestone Accomplishments

Milestone 3.3: Acceptance into peer-reviewed journal was achieved through the acceptance of a manuscript and oral presentation at the 48th IEEE PVSC conference in late-June.

Milestone EOP-A: Modeled PV plant LCOE >20% reduction from baseline costs was partially achieved. While a full 20% reduction in plant LCOE was not seen through this analysis, significant LCOE reductions of 5-7% were observed in the optimized bifacial module and tandem module cases analyzed.

Milestone EOP-B: Published optimization code was achieved through the public publication of the optimization algorithm developed for this research to GitHub (https://github.com/epri-dev/PV-PySAM-Optimization). Step-by-step instructions defining how to setup a new SAM model to work with the PySAM optimization algorithm are included with this publication.

Budget and Schedule:

This project ended on schedule and within budget. The project spanned one budget period beginning April 30, 2020 and ending June 30, 2021, with a small amount of spending occurring in the following three months as final report materials were prepared. The project spent $248,639 against a project plan of $249,957, with 80% federal share and 20% cost share from EPRI. The slight difference between planned and actual budget is due to unused travel budget as a result of travel restrictions due to the pandemic.

Path Forward:

EPRI continues to seek opportunities to share results and insights from this effort with EPRI utility members and the PV community as a whole through webcasts and meeting presentations. Discussions are underway both internally at EPRI and with utility stakeholders about how the methodology and optimization algorithm developed through this project can be applied to future research needs, including analyzing PV plant design tradeoffs for existing and new technologies and/or novel plant characteristics. All of these efforts will help to continue to advance the deployment of solar PV technologies in a cost effective and efficient manner.

Inventions, Patents, Publications, and Other Results:

A manuscript and oral presentation focusing on the bifacial module optimization results of this research was developed and presented virtually for the 48th IEEE PVSC. The manuscript, *Techno-economic Analysis of Novel PV Plant Designs for Extreme Cost Reductions,* can be found at the following link: https://ieee-pvsc.org/ePVSC/manuscripts/PVSC-355-0630081407.pdf

References:

1. M.T. Patel, M. Ryyan Khan, X. Sun and M.A. Alam “A Worldwide Cost-based Design and Optimization of Tilted Bifacial Solar Farms.” Applied Energy (Volume: 247). August 2019.
2. M.T. Patel, R. A. Vijayan, R. Asadpour, M. Varadharajaperumal, M. Ryyan Khan, and M. A. Alam. “Temperature Dependent Energy Gain of Bifacial PV Farms: A Global Perspective.” Applied Energy. vol. 276. October 2020.
3. B. Marion, S. MacAlpine, C. Deline, A. Asgharzadeh, F. Toor, D. Riley, J. Stein, C. Hansen. “A Practical Irradiance Model for Bifacial PV Modules.” National Renewable Energy Laboratory (NREL). June 2017.
4. *LONGi releases “Technical Brief” for its new Hi-MO 5 module for ultra-large power plants*. LONGi Solar. June 2020. https://en.longi-solar.com/home/events/press_detail/id/247_LONGi_releases_Technical_Brief_for_its_new_Hi-MO_5_module_for_ultra-large_power_plants.html
5. *Canadian Solar Launches Series 7 Modules of Up to 665 W.* CanadianSolar. October 2020. http://investors.canadiansolar.com/news-releases/news-release-details/canadian-solar-launches-series-7-modules-665-w
6. I. Etxebarria, A. Furlan, J. Ajuria, F. Fecher, M. Voigt, C. Brabec, M. M. Wienk, L. Slooff, S. Veenstra, J. Gilot, and R. Pacios. “Series vs parallel connected organic tandem solar cells: Cell performance and impact on the design and operation of

functional modules." Solar Energy Materials and Solar Cells (Volume: 130). November 2014.

7. T. White, N. Lal, and K. Catchpole. "Tandem Solar Cells Based on High-Efficiency c-Si Bottom Cells: Top Cell Requirements for >30% Efficiency." IEEE Journal of Photovoltaics (Volume: 4, Number 1). January 2014.
8. M. Hutchins. "Perovskite/silicon tandem solar cells approaching 30% efficiency in lab." PV Magazine. January 2020
9. G. Coletti, S.L. Luxembourg, L.J. Geerligs, V. Rosca, A.R. Burgers, Y. Wu, L. Okel, M. Kloos, F.J.K. Danzl, M. Najafi, D. Zhang, I. Dogan, V. Zardetto, F. Di Giacomo, J. Kroon, T. Aernouts, J. Hüpkes, C.H. Burgess, M. Creatore, R. Andriessen, and S. Veenstra. "Bifacial Four-Terminal Perovskite/Silicon Tandem Solar Cells and Modules." ACS Energy Letters 2020 5 (5), 1676-1680. April 2020.
10. S. Sofia, H. Wang, A. Bruno, J. Cruz-Campa, T. Buonassisi, and I. Peters. "Roadmap for cost-effective, commercially-viable perovskite silicon tandems for the current and future PV market". Sustainable Energy & Fuels. Vol. 2. February 2020.
11. R. West. "PV String to 3-Phase Inverter with Highest Voltage Capabilities, Highest Efficiency and 25 Year Lifetime." NREL. November 2011.
12. L. Scarpa, G. Chicco, F. Spertino, P. M. Tumino, and M. Nunnari. "Technical Solutions and Standards Upgrade for Photovoltaic Systems Operated Over 1500 Vdc". 2018 IEEE 4th International Forum on Research and Technology for Society and Industry (RTSI). September 2018.
13. C. Deline, J. Meydbray, M. Donovan, and J. Forrest. "Photovoltaic Shading Testbed for Module-Level Power Electronics." NREL. May 2012.
14. A. Elasser, M. Agamy, J. Sabate, R. Steigerwald, R. Fisher, and M. Harfman-Todorovic. "A comparative study of central and distributed MPPT architectures for megawatt utility and large scale commercial photovoltaic plants." IECON 2010 - 36th Annual Conference on IEEE Industrial Electronics Society. November 2010.
15. D. Vinnikov, A. Chub, E. Liivik, R. Kosenko, and O. Korkh. "Solar Optiverter—A Novel Hybrid Approach to the Photovoltaic Module Level Power Electronics." IEEE Transactions on Industrial Electronics (Volume: 66, Issue: 5). May 2019.
16. C. Lyons. "Solar Energy Technology Guide (3002003681)." Electric Power Research Institute (EPRI). December 2014.
17. H. Brent. "2016 Solar Energy Technology, Market, Cost, and Performance Report (3002008627)." EPRI. December 2017.
18. D. Feldman, T. Lowder, and P. Schwabe. "Terms, Trends, and Insights: PV Project Finance in the United States, 2016." NREL. September 2016.
19. D. Feldman and P. Schwabe. "Terms, Trends, and Insights on PV Project Finance in the United States, 2018." NREL. November 2018.
20. R. Bedilion. "2020 Solar Technology Status, Cost and Performance Report (3002018729)." EPRI. December 2020.

21. J. Lopez-Garcia, D. Pavenello, and T. Sample. “Analysis of Temperature Coefficients of Bifacial Crystalline Silicon PV Modules”. IEEE Journal of Photovoltaics, pp. 1-9. May 2018.
22. U. A. Yusufoglu, T. M. Pletzer, L. J. Koduvelikulathu, C. Comparotto, R. Kopecek, and H. Kurz. “Analysis of the Annual Performance of Bifacial Modules and Optimization Methods”. IEEE Journal of Photovoltaics. vol.5. November 2014.
23. C. Deline, J. Meydbray, M. Donovan, and J. Forrest. “Partial shade evaluation of distributed power electronics for photovoltaic systems”. NREL. June 2012.
24. X. Sun, M. R. Khan, C. Deline, and M. A. Alam. “Optimization and performance of bifacial solar modules: A global perspective.” Applied Energy. Vol. 212. February 2018.
25. M. Gul, Y. Kotak, T. Muneer, S. Ivanova. “Enhancement of Albedo for Solar Energy Gain with Particular Emphasis on Overcast Skies”. Energies. Vol. 11. October 2018.

Appendix A: Customized Component Specifications

Table 40: Comparison of Baseline Module and Custom Tandem Module Specifications.

Specification	Baseline Module (LONGi Solar LR6-72HPH-385M)	Custom Monofacial Tandem Module
Efficiency	19.3	26.5
Maximum Power (P_{mp})	384.7	528.9
Temp Coefficient of V_{oc} (%/°C)	-0.286	-0.208
Temp Coefficient of I_{sc} (%/°C)	0.057	0.057
Temperature Coefficient of P_{mp} (%/°C)	-0.37	-0.269
Module Area (m^2)	1.996	1.996
Maximum Power Voltage (V_{mp})	40.8	47.8
Open Circuit Voltage (V_{oc})	49.2	57.7
Maximum Current (I_{mp})	9.4	11.0
Number of cells in series	72	72
Short circuit voltage (I_{sc})	10	11.7
Nominal Cell Operating Temperature (°C)	45	45

Table 41: Custom Inverter Specifications Utilized for the Southwest Plant.

Southwest Plant				
Inverter Specifications	**Baseline (1500V)**	**2000V Custom Inverter**	**2500V Custom Inverter**	**3000V Custom Inverter**
Maximum AC Output Power (kW)	2500	3619	4314	4900
Manufacturer Efficiency (%)	98.6	98.6	98.6	98.6
Nominal AC Voltage (V)	550	733	917	1100
Maximum DC Voltage (V)	1500	2000	2500	3000
Maximum DC Current (A)	3200	3200	3200	3200
Minimum MPPT DC Voltage (V)	778	1037	1297	1556
Nominal DC Voltage (V)	1200	1500	1900	2300
Maximum MPPT DC Voltage (V)	1425	1900	2400	2900
Number of MPPT Inputs	1	1	1	1
Power Consumption during Operation (kW)	2.0	2.0	2.0	2.0
Power Consumption at night (kW)	0.370	0.370	0.370	0.370

Table 42: Custom Inverter Specifications Utilized for the Southeast Plant.

Southeast Plant					
Inverter Specifications	**Baseline (1000V)**	**Reference Inverter (1500V)**	**2000V Custom Inverter**	**2500V Custom Inverter**	**3000V Custom Inverter**
Maximum AC Output Power (kW)	24	125	204	243	276
Manufacturer Efficiency (%)	98.5	98.5	98.5	98.5	98.5
Nominal AC Voltage (V)	480	480	640	800	960
Maximum DC Voltage (V)	1000	1500	2000	2500	3000
Maximum DC Current (A)	66	180	180	180	180
Minimum MPPT DC Voltage (V)	450	705	940	1175	1410
Nominal DC Voltage (V)	1000	1100	1500	1800	2200
Maximum MPPT DC Voltage (V)	800	1450	1900	2400	2900
Number of MPPT Inputs	2	1	1	1	1
Power Consumption during Operation (kW)	0	0	0	0	0
Power Consumption at night (kW)	0.0072	0.005	0.005	0.005	0.005

Table 43: Custom Inverter Specifications Utilized for the Midwest Plant.

Midwest Plant				
Inverter Specifications	**Baseline (1500V)**	**2000V Custom Inverter**	**2500V Custom Inverter**	**3000V Custom Inverter**
Maximum AC Output Power (kW)	250	353	421	478
Manufacturer Efficiency (%)	99	99	99	99
Nominal AC Voltage (V)	800	1067	1333	1600
Maximum DC Voltage (V)	1500	2000	2500	3000
Maximum DC Current (A)	312	312	312	312
Minimum MPPT DC Voltage (V)	860	1147	1433	1720
Nominal DC Voltage (V)	1160	1600	2000	2400
Maximum MPPT DC Voltage (V)	1300	1900	2400	2900
Number of MPPT Inputs	12	9	9	9
Power Consumption during Operation (kW)	0	0	0	0
Power Consumption at night (kW)	0.002	0.002	0.002	0.002

Table 44: Enphase IQ7A Microinverter Specifications.

Specification	IQ7A Microinverter Case
Maximum AC Output Power (kW)	349
Manufacturer Efficiency (%)	97
Nominal AC Voltage (V)	240
Maximum DC Voltage (V)	58
Maximum DC Current (A)	15
Minimum MPPT DC Voltage (V)	18
Nominal DC Voltage (V)	33
Maximum MPPT DC Voltage (V)	58
Number of MPPT Inputs	1
Power Consumption during Operation (kW)	--
Power Consumption at night (kW)	--